B. TECH. PROJECT REPORT

On

Assessment of Flexible Pavement on Expansive Soil

BY

Divya Sharma

160004014

DISCIPLINE OF CIVIL ENGINEERING

INDIAN INSTITUTE OF TECHNOLOGY INDORE

December 2019

Assessment of Flexible Pavement on Expansive Soil

A PROJECT REPORT

Submitted in partial fulfillment of the requirements for the award of the degrees

of
BACHELOR OF TECHNOLOGY
in
CIVIL ENGINEERING

Submitted by:
Divya Sharma (160004014)
Guided by:
Dr. Neelima Satyam
Associate Professor, Discipline of Civil Engineering, IIT Indore

INDIAN INSTITUTE OF TECHNOLOGY INDORE
December 2019

CANDIDATE’S DECLARATION

We hereby declare that the project entitled **“Assessment of Flexible Pavement on Expansive Soil”** submitted in partial fulfillment for the award of the degree of Bachelor of Technology in ‘Civil Engineering’ completed under the supervision of **Dr. NEELIMA SATYAM,** Associate Professor, Discipline of Civil Engineering, IIT Indore is an authentic work.

Further, I declare that I have not submitted this work for the award of any other degree elsewhere. degree elsewhere.

Divya Sharma

CERTIFICATE by BTP Guide(s)

It is certified that the above statement made by the students is correct to the best of my/our knowledge.

Signature of BTP Guide(s) with dates and their designation

Preface

This report on **Assessment of Flexible Pavement on Expansive Soil"** is prepared under the guidance of Dr. Neelima Satyam, Associate Professor, Discipline of Civil Engineering, IIT Indore

Through this report I have presented the difference between reinforced and unreinforced flexible pavement on expansive soil. Geotextile and Geogrid are used for the same.

The simulated results shown in the report are obtained by using Abaqus Unified FEA.

Divya Sharma
B.Tech. IV Year
Discipline of Civil Engineering
IIT Indore

Acknowledgements

I would like to express my sincere and deepest gratitude to my final year B.Tech. project supervisor Dr. Neelima Satyam for her kind support and valuable guidance. I have gained a lot through the interaction with her during the project work.

I am also greatly indebted to Mr. Nitin Sharma, PhD scholar for guiding me along all difficulties and helping me to make the project reality. His sound advice and insights helped me to put my best step forward.

I would also like to thank my parents for their unwavering support and encouragement. It is their help and support, due to which I became able to complete the project and able to form report.

I would like to acknowledge IIT Indore for providing all necessary research infrastructures required for undertaking the project.

Divya Sharma
B.Tech. IV Year
Discipline of Civil Engineering
IIT Indore

Abstract

Transportation agencies encounter considerable challenges when they deal with expansive soils underneath roadway structures. Due to swelling shrinkage nature of expansive soil, structure experience high Upward swelling pressure. India covers 15%-20% area with expansive soil which causes severe damage to existing structures including paved structures, dams, multi-storey buildings, retaining walls, etc. The various conventional mechanical and chemical treatment methods developed to counteract the effect on expansive soil subgrade, which are time consuming and not feasible to use for the paved structure construction. This project deals with the effect of single, double and triple layer synthetic geotextile at varying depth to stabilize the expansive soil subgrade and with the effect single layer of geogrid placed at different depths to provide better reinforcement to base layer of Flexible Pavement. The constant volume swelling pressure, California bearing ratio (CBR), and Unconfined Compression (UCS) test were carried out to evaluate the efficiency of geotextile and geogrid for increasing bearing capacity of expansive soil subgrade. CBR is performed on hybrid structure also containing both Geotextile and Geogrid in subgrade and base layer respectively. The experimental results analyzed with the inclusion of synthetic geotextile in expansive soil subgrade, indicates that Swelling pressure is decreased and the bearing strength is increased in the presence of Geotextile. The tangible improvement in the stress strain behavior and bearing capacity of pavement is observed with synthetic geotextile and Geogrid Layer.

Numerical Analysis using the finite element approach was also conducted on hybrid pavement to validate that the deformation and rutting in a pavement is under the permissible values according to MoRTH (Ministry of Road Transport and Highway) and IRC 37:2012. It is observed that usage of geosynthetic gives result in permissible range only with less error between numerical and experimental values.

Table of Contents

Chapter 1 Introduction 11
1.1 Flexible Pavement 12
1.2 Expansive Soil 13
1.3 Problem Statement 14
1.4 Scope 16
1.5 Objective 18
1.6 Organization of thesis 18
Chapter 2 Work Flow of Thesis 20
Chapter 3 Literature Review 23
3.1 Expansive Soil Stabilization 23
3.1.1 Chemical Stabilization 23
3.1.2 Mechanical Stabilization 23
3.2 Use of Geosynthetic (Geotextile and Geogrid) 24
3.2.1 Geotextile 24
3.2.2 Geogrid 24
3.3 Numerical Modeling 25
3.4 Research Gap 25
Chapter 4 Material 26
4.1 Aggregate 26
4.2 Expansive Soil 27
4.2.1 Attenberg Limit Test 27
4.2.2 Moisture-Density relationship 27
4.2.3 Free Swell Index Test 27
4.2.4 Hydrometer Analysis test 28
4.3 Geotextile 28
4.4 Geogrid 29
Chapter 5 Experimental Performance 31
5.1 Cases with Different Position of Geotextile and Geogrid 31
5.1.1 CBR Test 32
5.1.2 Constant volume Swelling Pressure Test 34
5.1.3 Unconfined Compression Test 35
5.2 Results and Discussion 36
Chapter 6 Numerical Performance Evaluation 46

6.1 Geometry 47
6.2 Material Model 48
6.2.1 Linear Elastic Model 48
6.2.2 Mohr Coulomb Model 49
6.2.3 Sorption Model 50
6.2.4 Moisture Swelling Model 51
6.2.5 Permeability Model 51
6.3 Interaction Model 51
6.4 Boundary Condition 52
6.5 Mesh Size 53
6.6 Load Condition 53
6.7 Validating Deformation Behavior 54
Chapter 7 Result and Validation for Rutting Failure 58
Chapter 8 Conclusion and Future Work 600
8.1 Conclusion 60
8.2 Future work 61
Publications 62
References 63

List of Figures

Fig1. 1 Flexible Pavement 13

Fig1. 2 Map of soil distribution in India 14

Fig1. 3(a) Alligator Cracking (b) Potholes in Flexible Pavement 15

Fig1. 4 Swelling and Shrinkage of Expansive Soil.. 15

Fig1. 5(a) longitudinal crack developed on pavements over expansive clays (b)Rutting Distress 16

Fig1. 6 Function of Geosynthetic.. 17

Fig1. 7 Function of Geogrid... 18

Fig.4. 1 (a) Geotextile (b) Geogrid 30

Fig.5. 1 Various Geotextile Depths considered for experimental work (h=height of apparatus of experiment) 31

Fig.5. 2 Various Geogrid and Geotextile Depths considered for experimental work (h=height of soil layer and H is height of aggregate layer of apparatus of experiment) 32

Fig.5. 3 Top view of CBR mould with Geotextile at top.. 34

Fig.5. 4(a) Top view of mould with Geotextile at top, (b) Test apparatus 35

Fig.5. 5 UCS mould ready to test... 36

Fig.5. 6 Graph of Swelling Pressure vs time 37

Fig.5. 7 Box Plot to show the variation in swelling Pressure 38

Fig.5. 8 Graph of Percentage swell for unreinforced and reinforced section 39

Fig.5. 9 Box plot for the percentage swell for unreinforced and reinforced section 39

Fig.5. 10 Time ratio plot for various cases 40

Fig.5. 11 Effect of Geotextile layer on swelling pressure and percentage swell ratio.................. 41

Fig.5. 12 Graph shows the change in CBR values for reinforced and unreinforced cases 43

Fig.5. 13 Graph shows CBR value of unreinforced and reinforced case with Geogrid and Geotextile.. 43

Fig.5. 14 Axial stress-strain curve of reinforced and unreinforced expansive soil....................... 44

Fig.5. 15 UCS deformation behavior of reinforced and unreinforced expansive soil 45

Fig 6. 1 Geometry of the model 47
Fig 6. 2 Mesh size for (a) Agg. + BC + GG(h0) + GT(H0), (b) Agg.+ BC + GT(H0), (c) Agg.+ BC + GT(H4) and (d) Agg. + BC + GG(h2) + GT(H0) 53
Fig 6. 3 Model after applying Load and Boundary Conditions 54
Fig 6. 4 Strain vs time Graph of (a) Agg. + BC + GG(h2) + GT(H0), (b) Agg. + BC + GG(h0) + GT(H0), (c) Agg.+ BC + GT(H4) and (d) Agg. + BC + GT(H0) 55
Fig 6. 5(a),(b),(e),(f) shows the stress distribution and (c),(d),(g),(h) shows the strain distribution of base layer and subgrade layer for case(a) Agg. + BC + GG(h2) + GT(H0), (b) Agg. + BC + GG(h0) + GT(H0) respectively.. 56
Fig 6. 6(a),(b),(e),(f) shows the stress distribution and (c),(d),(g),(h) shows the strain distribution of base layer and subgrade layer for case(a)Agg.+ BC + GT(H4) and (b) Agg. + BC + GT(H0) 57

List of Tables

Table 4. 1 Properties of aggregate considered 26
Table 4. 2 Index Property of Expansive Soil considered 28
Table 4. 3 Index Properties of Geotextile considered 29
Table 4. 4 Index Properties of Geogrid Used 29

Table.6. 1 Input values for Linear Elastic Model 49
Table.6. 2 Input Values for Mohr Coulomb Model 50
Table.6. 3 Input values for Sorption Model 50
Table.6. 4 Input values for Moisture Swelling Model 51
Table.6. 5 The different interaction condition given at the interface 52

Table.7. 1 Experimental and Numerical Values for subgrade Layer 59

Chapter 1

Introduction

1.1 Flexible Pavement

Road and Highways sector is a significant part of construction industry where the exhaustive use of the natural resource has emerged as a severe threat to the environment (E.T.B.T.B. Edil, 2013). The reason for this is that the material procurement for construction, their extraction, and laying, generates a lot of pollution and waste. There are 2 types of Pavement for constructing a road, Flexible Pavement and Rigid Pavement. A flexible pavement can be considered as a multi-layered elastic structure constructed to provide a smooth movement of vehicle. Flexible Pavement comprises of three layers: Surface Layer, Base Layer and Subgrade Layers shown in Fig. 1.1. Under traffic loading, granular layer undergoes complex deformation behavior where large part consists of recoverable deformation and a small part is plastic or permanent deformation (Y. Huang, R.N. Bird, O. Heidrich, 2009). The plastic or permanent deformation accumulates with each load repetition and may eventually lead to rutting of the pavement (Uzan J., 2004; Cerni G et al, 2012). Apart from granular layer, subgrade soil also must be competent enough to resist the permanent deformation as stresses are finally transferred to the subgrade soil; however, of smaller magnitude as compared to the granular layer. Several research studies have been conducted to investigate the permanent deformation behavior of subgrade soil under cyclic loading [22–26](Li D, Selig ET, 1996; Puppala AJ et al, 1999; Puppala AJ, 2009; Chai J, Miura N., 2002; Lu Z et al, 2018). However, subgrade layer consisting of a clay soil/expansive soil is also a challenging part to deal with.

Most of the studies have been performed on material characterization and modeling of pavement layers. Therefore, pavement material of each layer and composite behavior of a whole structure are the big contributers in stress and strain response of a pavement.

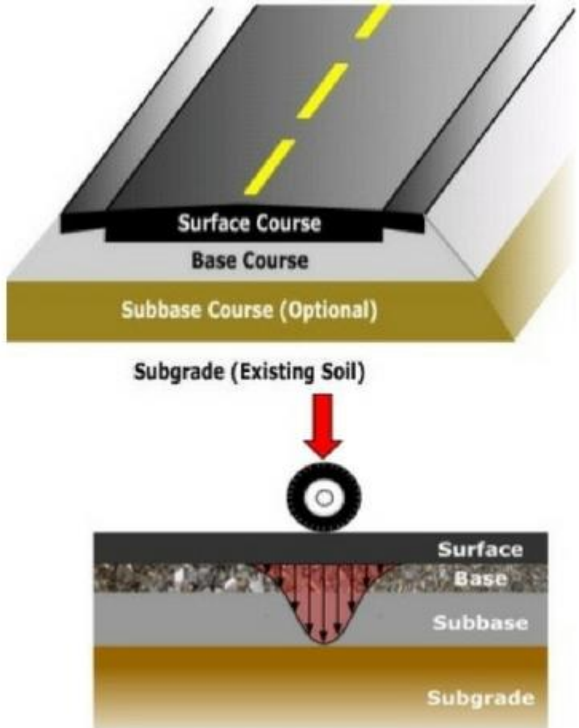

Fig1. 1 Flexible Pavement

1.2 Expansive Soil

Expansive soil is characterized by its nature of changing its volume with the change in water content. This change in a volume is known as swelling -shrinkage behavior of soil, and hence this soil is also known as swell-shrink soil (Jones et al., 1998; Phanikumar and Singla, 2016; Sivapullaiah et al., 1987; Sun et al., 2018). Soils with high plasticity contain clay minerals like Montmorillonite, which is hydrophobic in nature. Presence of such mineral is one of the biggest reasons of such soil exhibiting high swelling nature in the presence of water content.

Pavement distresses in roadways is one of the impacts of the presence of expansive soil in the subgrade layer (Marradi et al., 2012; Samer et al., 2012; Srivastava et al., 2018). In dry state, soil initiate shrinkage cracking, which propagates through the pavement system and leads to longitudinal, transverse and fatigue cracking and rutting in the case of pavement surface (Kermani et al., 2018). Structures also suffer comparatively extensive damage when constructed on highly plastic clay subgrade as such soils undergo cycles of wetting and drying. Therefore, such characteristics of expansive fine-grained soil are one of the most significant reasons which lead to cracks, distress and most of the damage (Camacho-Tauta et al., 2016) .

Expansive soil lies mostly in the central and the western part and covers more than 15% of the geographical area of India as can be seen from Fig.1.2. (Thirumalai et al., 2017). The expansive soil subgrade swell during rain and shear failure in the structure occurred. Various mechanical and chemical methods were lingering to mitigate the swelling pressure and heave phenomena of the expansive soil. Mechanical (Hammouri et al., 2008; Punthutaecha et al., 2006; Tinoco et al., 2016) and chemical (Akinwumi and Ukegbu, 2015; Estabragh et al., 2014; Krause Sternberg, 1977; Phanikumar and Nagaraju, 2018; Sharma et al., 2019; Shukla et al., 2018) stabilization are the conventional methods used to improve the engineering properties of expansive soils; however, these methods are time-consuming and uneconomical.

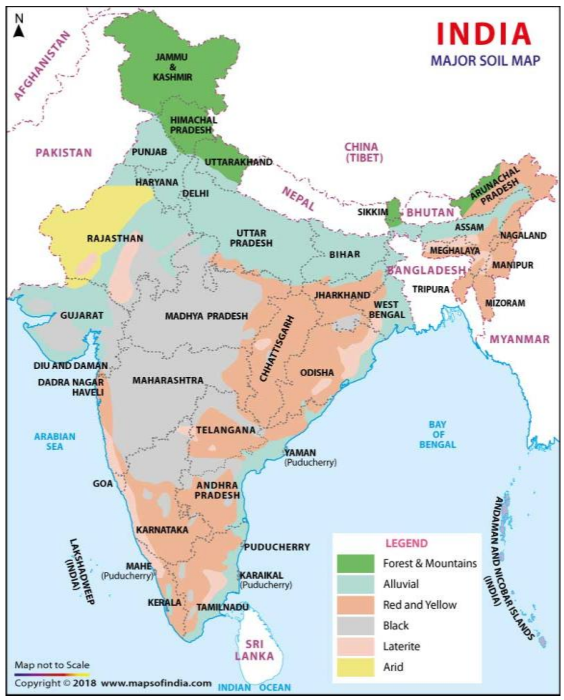

Fig1. 2 Map of soil distribution in India

1.3 Problem Statement

Problem with Flexible Pavement having Expansive Soil Subgrade:

i) Cracking, Deformation, Deterioration: These are the most common problems that can be observed on the surface layer, but its origin can be subgrade layer too.

 

Fig1. 3(a) Alligator Cracking (b) Potholes in Flexible Pavement

ii) Major cause of failure of Flexible Pavements are:

- Relative Movement of pavement layer material
- Repeated Application of Heavy loads

The volume Change in expansive soil can either be in the form of swelling or in the form of shrinkage, due to its mineralogy. This swelling shrinkage behavior is not recurring at regular interval of time. So measures to prevent the structures present above expansive soil have to be related to stabilization of soil rather than just taking precaution at a particular time of occurrence.

Fig1. 4 Swelling and Shrinkage of Expansive Soil

(a) (b)

Fig1. 5(a) longitudinal crack developed on pavements over expansive clays (b)Rutting Distress

Stabilization of Expansive soil is affected because of some phenomena like:

i) The clay mineralogies

ii) The stress histories of the soil masses

iii) The weather condition where these soils are found

iv) The property changes in these soils with time

(Thomas M. Petry and J. Clyde Armstrong,2008)

So, the stabilization approaches adopted were chemical and mechanical stabilization. The problems faced with these methods were:

i) The chemical stabilization process of expansive soil subgrade is time consuming and uneconomical.

ii) Mechanical Method required large scale energy to compact and is only efficient for the low depth.

iii) Mixing of any material and chemical for the flexible is not much suitable, due to large length.

1.4 Scope

The scope left after mechanical and chemical stabilization process is to carry out the performance evaluation of geosynthetic (geogrid and geotextile) reinforced sub-grade of flexible pavement by detailed experimental and numerical studies.

Field evidence and theoretical studies have indicated that the service life of flexible pavements can be extended by installing nonwoven geotextiles or geogrids between the existing layer and the new developed layer due to the ability of the geosynthetic to minimize the development of reflective cracks (Lytton 1989; Austin and Gilchrist 1996; Prieto et al. 2007; Virgili et al. 2009; Yu et al. 2013; Khodaii et al. 2009; Fallah and Khodaii 2015; Gonzalez-Torre et al. 2015).

The Main Functions of Geosynthetic are as follow:

i) Holding and capturing the aggregates together.
ii) Used for load distribution, soil separation, filtration, reinforcement and drainage.
iii) Improvement in bearing capacity of subgrade layer.
iv) Reduction in shear stresses and strains on the top of subgrade layer.

The Main Functions of Geogrid are as follow:

i) Stabilized mechanically by Interlocking the aggregate
ii) Reinforce Subbase below roads
iii) Increases tensile Strength
iv) helps in redistribution of load over a wider area

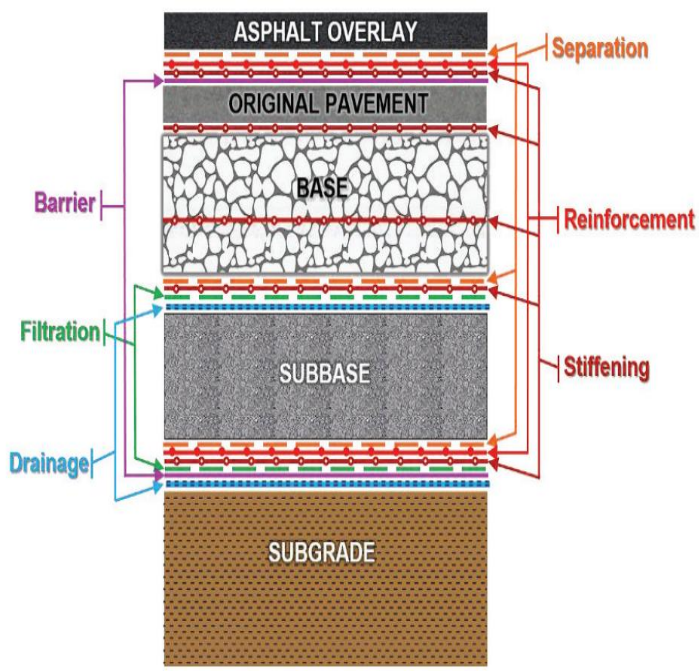

Fig1. 6 Function of Geosynthetic

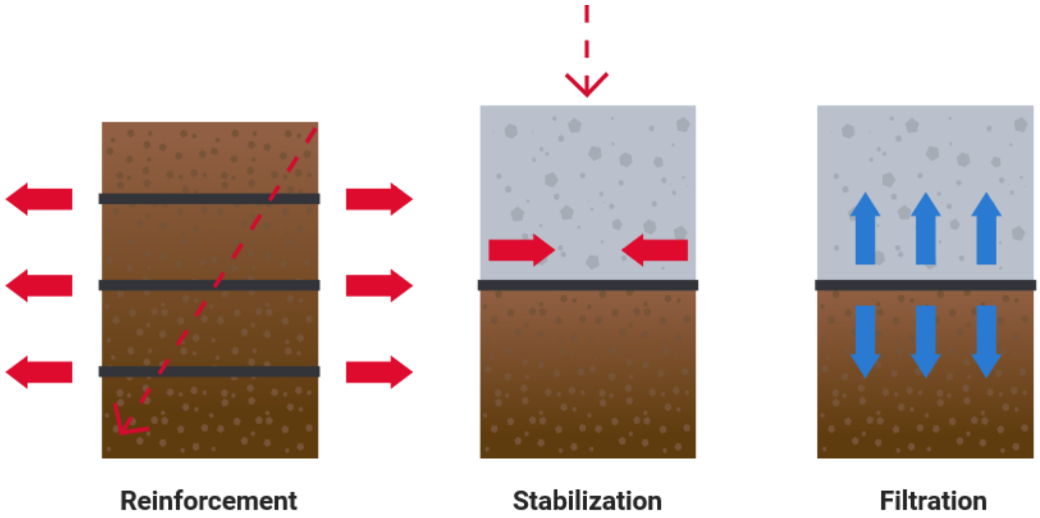

Fig1. 7 Function of Geogrid

1.5 Objective

The objectives of my research project are:

i) To utilize the geosynthetic for stabilizing sub-grade layer of flexible pavement

ii) To analyze subgrade deformation behavior of sub-grade flexible pavement

iii) To evaluate the performance of modified pavement system

iv) To investigate the flexible pavement's deformation behavior using numerical method.

1.6 Organization of thesis

Chapter 2 outlines in detail the flow of the work done to assess the properties of subgrade layer with reinforced and unreinforced soil foundation and bases in flexible pavement.

Chapter 3 presents an extensive literature review of various methods of Expansive soil stabilization and finally the review of experimental and numerical studies of reinforced and unreinforced subgrade layer and base layer. Focus is given to the geosynthetic use and its results reported by other researchers.

Chapter 4 comprises of the material properties of the soil, aggregate, Geotextile and Geogrid. The property of Geotextile and Gogrid is provided by the supplier that are tested according to the various codes. Aggregate and soil that is used are tested in laboratory to do the material property analysis.

Chapter 5 comprises of experimental tests which are done for the engineering property analysis of the reinforced and unreinforced subgrade layer.

Chapter 6 presents the details of the numerical modeling and the effort undertaken for that during research.

Chapter 7 presents the results from experimental and numerical modeling and then the validation done for these values according to IRC37:2012.

Chapter 8 summarizes the findings and concludes, with the help of the results obtained. This chapter also provides some suggestions for future work.

Chapter 9 shows the publication done while doing the research.

Chapter 2

Work Flow of Thesis

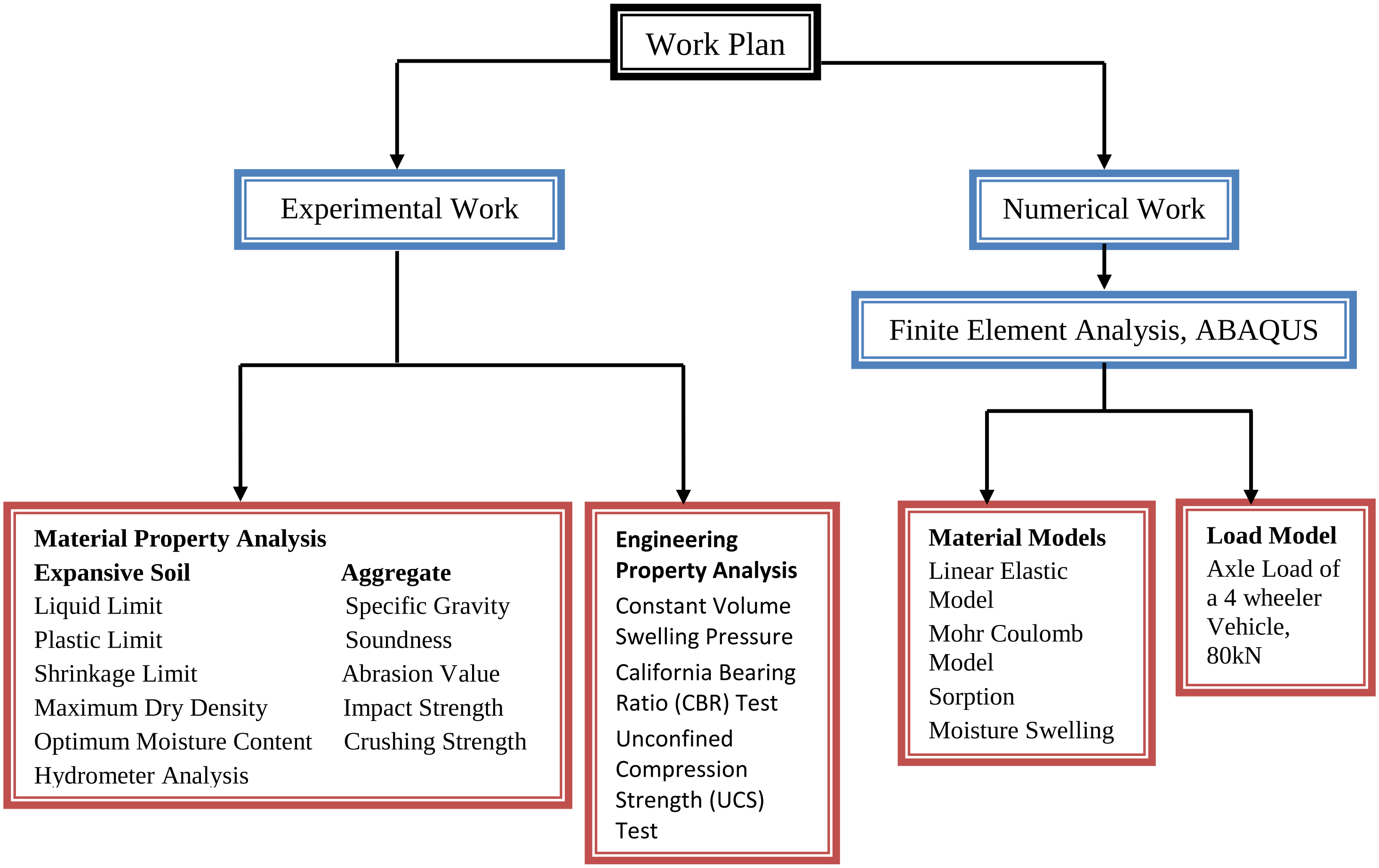

Fig 2. 1 Flow chart of work plan for this thesis

The above flow chart shows the various tests that are performed to analyze the expansive soil behavior present in subgrade layer in flexible pavement.

First, the Experimental work is performed. In this Basic test for Material Property Analysis is done with the help of various tests like Liquid Limit Test, Plastic Limit Test, Shrinkage Limit Test, Maximum Dry Density, Optimum Moisture Content and Hydrometer Analysis for Expansive soil; and Specific Gravity, soundness, Abrasion value, impact Strength and crushing strength for Aggregate. After that, tests to know the engineering property of subgrade layer containing soil and also the difference in engineering property of layer when the Geotextile is included in the soil at different position. Engineering property analysis includes Constant Volume Swelling pressure test, CBR test and UCS test. Each test is performed 15 times having Geotextile at different depths. CBR is performed 6 times more with Geogrid and Geotextile both in base and subgrade layer respectively at different positions. The value obtained by each test is the mean value of the three tests that are performed in similar condition only as it reduces the chance of error.

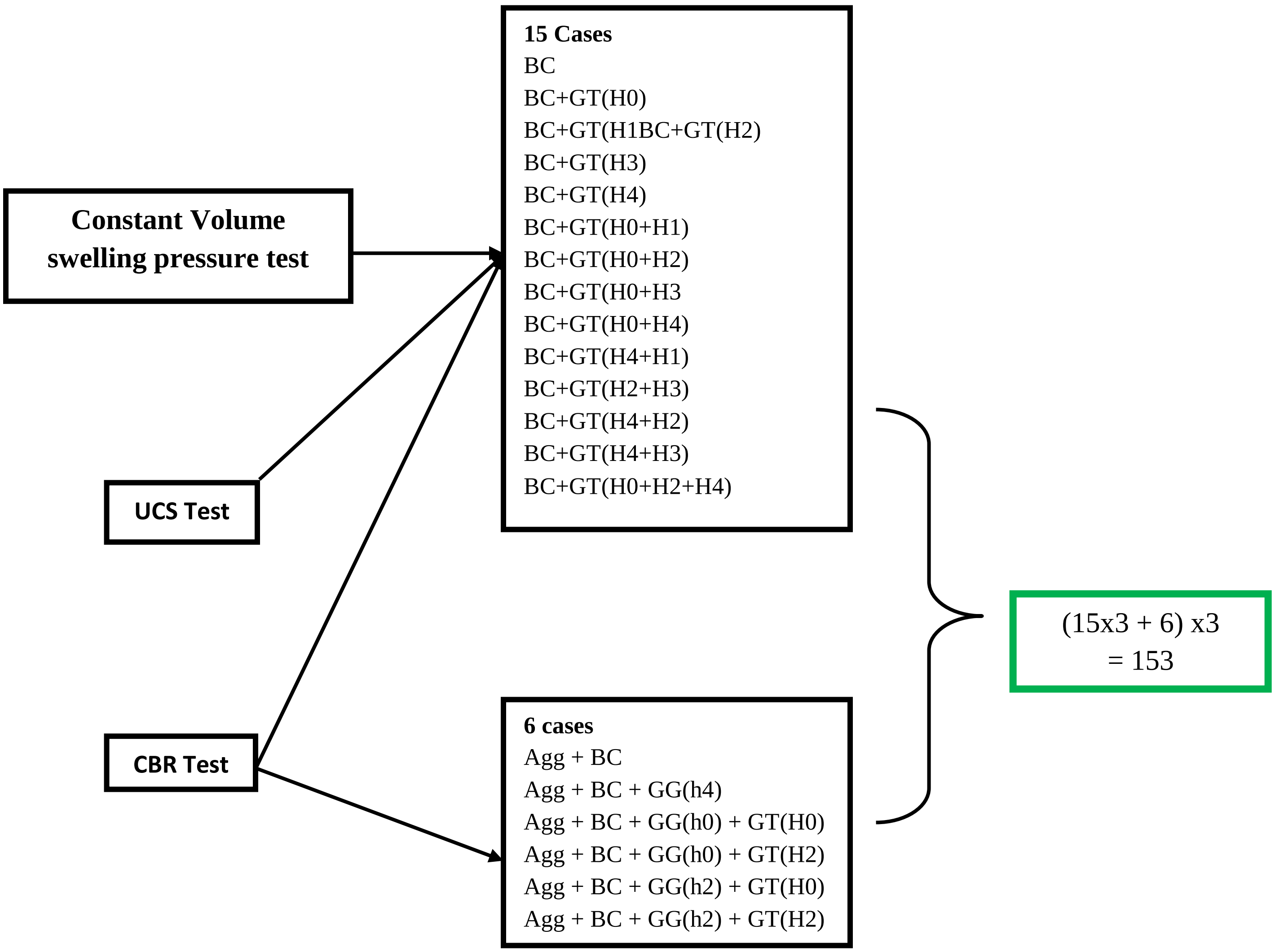

Fig 2. 2 Experiments with different cases

Second, the Numerical work is done with the help of software, known as ABAQUS. In this numerical model, inputs are given according to the experimental results. Various models like Material model, Interaction, Boundary condition, Load model, etc plays a great importance in getting the accurate results of stress and strain. These results finally helps in design of the pavement by validating that use of geosynthetic is useful as well as the deformation and rutting are in the permissible range.

Chapter 3

Literature Review

3.1 Expansive Soil Stabilization

This chapter presents a summary of the published literature on expansive soils and associated problems along with the current remedial approaches and their limitations to mitigate these problems. Due to such nature of soil, i.e., Swelling and Shrinkage, various stabilization methods have been tried. The 2 stabilization methods were (Thomas M. Petry and J. Clyde Armstrong):

3.1.1 Chemical Stabilization

Chemical Stabilization is the initial method use to change the mineral composition of the soil in order to control the swelling behavior. Probably the most effective chemical stabilization of expansive clays occurs when the cations present in the natural clay are exchanged for bivalent or with low affinities for water. Initially, 2 % hydrated lime was first used by corps of engineers (U.S.A- 1943) to reduce the plasticity index at chase field in Texas. But problem faced in this stabilization is that, the chemical stabilization process of expansive soil subgrade is time consuming and uneconomical as mixing chemicals to the soil at large scale is not a easy task. (Akinwumi and Ukegbu, 2015; Estabragh et al., 2014; Krause Sternberg, 1977; Phanikumar and Nagaraju, 2018; Sharma et al., 2019; Shukla et al., 2018)

3.1.2 Mechanical Stabilization

Mechanical Stabilization includes tests on expansive soil reinforced with randomly distributed fibres which results in mechanical improvement with different percentages, and different lengths. This method is adopted as in the design process of layers, no stabilizing agent is used, it builds something over the movements expected of the expansive soil mass. But this method required large scale energy to compact and is only efficient for the low depth. (Hammouri et al., 2008; Punthutaecha et al., 2006; Tinoco et al., 2016)

These are the 2 conventional method used to improve the engineering properties of soil. But eventually with time, we understand that mixing of any material and chemical for the flexible is not much suitable, due to large length.

3.2 Use of Geosynthetic (Geotextile and Geogrid)

Reinforcement geosynthetics are used for different applications in geotechnical engineering such as reinforced earth fills, retaining walls, embankments, road pavement and foundations (Mahmoud G. Hussein & Mohamed A. Meguid, 2013). Geosynthetic has now emerged as one of the cost-effective and sustainable construction materials as Separation, Filtration, Reinforcement, and Stiffening are some of the primary function which can be used to enhance the engineering properties of the subgrade layer (Cristelo et al., 2016; Onur et al., 2016; Peng and Zornberg, 2017; Perkins and Ismeik, 1997; Vieira and Pereira, 2016; Zornberg, 2017; Baek and Al-Qadi 2006).

3.2.1 Geotextile

Installing geotextile led to the extension of the service life of the pavement due to its ability to minimize the development of reflective cracks and also reduce the chances of cracks by reducing the expansion and shrinking of the subgrade layer as indicated by various field evidence and theoretical studies of geotechnical engineers (Consoli et al., 2011; Mazzoni et al., 2017a; Sina Mirzapour Mounes et al., 2011; Nejad et al., 2008; Tiwari and Satyam, 2019; Zornberg, 2012). Among the different forms of Geosynthetic, geotextile has property of high tensile strength, to provide separation, frictional resistance to stabilize the soft soil subgrade (Palmeira et al., 2009).

3.2.2 Geogrid

Geogrid is the type of polymeric geosynthetics that is designed specifically to provide reinforcement to the soil. Geogrid is the three-dimensional open structure, has a special property of interlocking with the surrounding material. Because of such special characteristics, it creates a cost effective earth structure (Koerner, 1994; Mir Md. Tamim, 2017; Hema Siriwardane et al., 2008).

3.3 Numerical Modeling

Finite Element Analysis for a pavement has been conducted with ABAQUS in many research Papers in order to obtain the stress and strain pattern in different layers. Three-dimensional models give more accurate results for pavement response. But attention must be given to the material properties, interactions and the ability of the selected material model to accurately predict responses (Beena Sukumaran et al., 2013; Fan Gu, et. al.2016; Stefan A. Romanoschi and John B. Metcalf,2009; Beena Sukumaran, 2004) . They have used Geosynthetic also at various positions to analyse the effect of such changes in stress and strain. Various methods to apply load, like by giving axle load, cyclic load, considering imprint of tyres, etc are also considered (Rahman M.T, 2011; Muhammad N.S. Hadi, B.C. Bodhinayake , 2003; Stefan A. Romanoschi and John B. Metcalf,2009) . It was observed that inclusion of Geotextile and Geogrid reduces the stress and strain in layers.(Hema Siriwardane ,Raj Gondle Bora Kutuk, 2010; (Vahid Rashidian et al.,2016; Li Liu,2008)

3.4 Research Gap

Several Researchers studied the effect of geotextile to use as a filtration media; however, the effect of geotextile on swelling pressure and bearing capacity has not given much importance. Therefore, this research focuses on the use of geotextile in subgrade layer and geogrid in base layer to investigate its effect on swelling pressure, CBR and unconfined compressive strength property of expansive soil subgrade.

Chapter 4

Material

4.1 Aggregate

The Aggregates used in this study is considered as the crushed quartz aggregates. Various lab experiments are performed to know the properties of Aggregates. Some of the tests are Grain size distribution test, Specific Gravity, soundness, Abrasion value, impact Strength and crushing strength. The Experimental results obtained from the laboratory experiments are given in the table given below. The gradation curve obtained experimentally is compared with MoRTH limits for the flexible paved structure construction which implies that aggregate is grade II material.

Test Parameters	Specified Limit (MoRTH)	Test Result	Test Method
Bulk specific gravity	2-3	2.49	IS 2386
Percent wear by Los Angles abrasion (%)	Max 35%	10.3	IS 2386
Soundness Loss by sodium sulfate solution (%)	Max 12%	3	IS 2386
Soundness Loss by magnesium sulfate solution (%)	Max 18%	3.3	IS 2386
Flaky elongation Index (%) **20mm** **10mm**	Max 35%	 27.93 32.13	IS 2386
Impact Strength (%) **20mm** **10mm**	Max 27%	 4.15 5.91	IS 2386
Water Absorption (%)	Max 2%	1.76	IS 2386
Water Sensitivity (%)	Min 80%	95	AASHTO 283

Table 4. 1 Properties of aggregate considered

4.2 Expansive Soil

The Expansive clay soil used in this study was taken from Indore (India) at a depth of 1.5m - 2m from the surface. To characterize the soil sample, various tests were conducted like Atterberg Limit Test, moisture-density relationship , Free Swell Index Test and Hydrometer Analysis Test

4.2.1 Atterberg Limit Test

Atterberg Limits are an index of soil consistency. It is the basic measure of critical values of \ water content like Liquid Limit (LL) and Plastic Limit (PL) in soil. The LL is where the soil changes from a liquid to plastic state and PL is where the soil changes from a plastic to a semisolid state (ASTM D4318). Plasticity Index (PI) is the Difference between LL and PL. It tells about the plasticity of soil. Soil sample taken for the test is oven dried (105^0) followed by passing through #40 sieve. The test for LL and PL is performed according to ASTM D4318. It is observed that PI of the soil sample is greater than 35, so it is observed that soil is highly expansive in nature.

4.2.2 Moisture-Density relationship

The optimal moisture content (OMC) at which soil can reach its maximum dry density (MDD) is obtained. Proctor compaction is done to obtain these values. The test is conducted according to ASTM D698. A curve is plotted between dry unit weight and moisture content of the soil, which also shows the OMC and MDD values.

4.2.3 Free Swell Index Test

Free swell index is the percentage increase in the volume of soil when submerged in water without any external pressure. This test is conducted according to IS: 2720-1977. This value is defined as:

$$\text{Free Swell Index} = \frac{V_d - V_k}{V_k} \times 100\%.$$

4.2.4 Hydrometer Analysis test

Hydrometer Analysis is done on a fine grained soil and whose gradation is less than No. 200 (.075mm). Type 151H hydrometer is used for analysis. The test was conducted according to ASTM D7928-17. In this analysis, portion of Clay and Silt in soil is determined.

S.No.	Property	Value
1.	Specific Gravity	2.78
2.	Liquid Limit(%)	89
3.	Plastic Limit(%)	47
4.	Plastic Index(%)	42
5.	Shrinkage Limit(%)	11
6.	USCS soil Classification	CH
7.	Grain Size Distribution	
	Clay(%)	71.5
	Silt(%)	24.5
8.	Free Swell Index(%)	120

Table 4. 2 Index Property of Expansive Soil considered

4.3 Geotextile

Tencate Geotextile, Hyderabad provided us the geotextile used in the project. The geotextile used has a high tensile strength of 28kN/m, Tensile Elongation of 80/40mm (MD/CD), with the CBR Puncture strength of 4250kN/m. Its effective opening size, Nominal Mass and Thickness is 0.08mm, 400gm and 3.2mm respectively. Test Standards follow IS codes and ASTM codes

Property	Test Standard	Unit	Values
UV Resistance			
tensile strength retention	ISO 10319	%	>70
puncture strength retention	ISO 12236	%	>70
Tensile strength(av.)	ISO 10319	kN/m	28
Tensile elongation(MD/CD)	ISO 10319	%	80/40
Performance Energy	Calculated	kN/m	8.4
CBR Puncture strength	ISO 12236	N	4250
Effective opening size O_{90}	ISO 12956	mm	0.08
Vertical water flow(50mm head)	ISO 11058	$l/m^2/s$(mm/s)	50
Horizontal water flow(20kPa)	ISO 12958	l/m.h	20
Horizontal water flow(200kPa)	ISO 12958	l/m.h	4.0
Nominal Mass	ISO 9864	g/m^2	400
Thickness(2kPa)	ISO 9863	mm	3.2
Grab Strength(MD/CD)	ASTM D4632	N	1770/1650
Grab Elongation(MD/CD)	ASTM D4632	%	75/40
Apparent opening size O_{95}	ASTM D4751	mm	0.15
Permittivity	ASTM D4491	s^{-1}	1.7

Table 4. 3 Index Properties of Geotextile considered

4.4 Geogrid

The Geogrid used in the project was provided by Tencate Geosynthetics, Secunderabad, Telangana, India. The Geogrid used has a Ultimate Tensile Strength of 51.1kN/m, Tensile Strength at 5% strain of 15.4kN/m, Creep Rupture Strength of 35.2kN/m and a Long Term Design strength of 30.5kN/m. Its mass/unit area is 251g/m^2. These values are according to the various tests results performed by following the Test Standards.

Properties	Test Standards	Unit	Values
Tensile Strength@Ultimate	ASTM D6637	kN/m	51.1
Tensile Strength @ 5% Strain	ASTM D6637	kN/m	15.4
Creep Rupture Strength	ASTM D5262	kN/m	35.2
Long Term Design Strength	ASTM D5261	kN/m	30.5
Mass/Unit Area		g/m^2	251

Table 4. 4 Index Properties of Geogrid Used

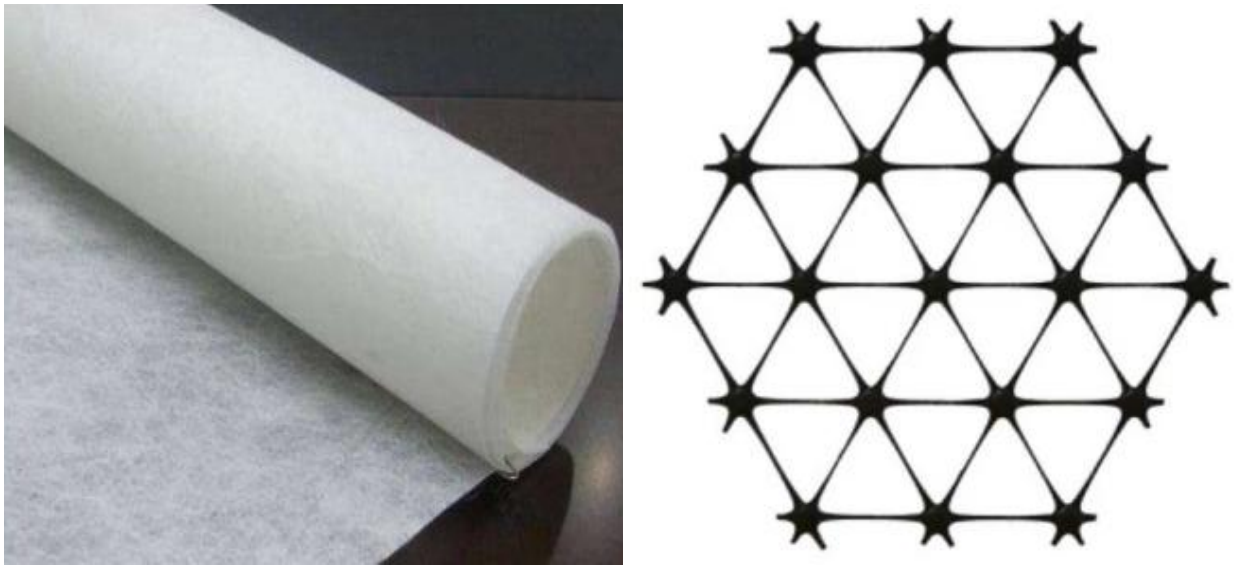

Fig.4. 1 (a) Geotextile (b) Geogrid

Chapter 5

Experimental Performance

5.1 Cases with Different Position of Geotextile and Geogrid

The design and construction of pavement over expansive soil is quite challenging and problematic for engineers. Such behavior of clayey soil like, high compressibility on load, swelling with respect to quantity of water content; affects mainly to the life of the pavement.
Such behavior can be controlled and its strength can be increased by introducing a geosynthetic Layer in subgrade layer and Base layer. In the available Literature Geogrids and Geosynthetics are popular as inclusion/reinforcement for improving engineering performance. In this Project, the experimental section has been divided in 15 test section by placing the synthetic geotextile layer at top, one third, half, two third and bottom of the soil specimen as shown in Fig.5.1. The synthetic geotextile layer has been placed at various depths to quantify the effect of placement position in the soil specimen.

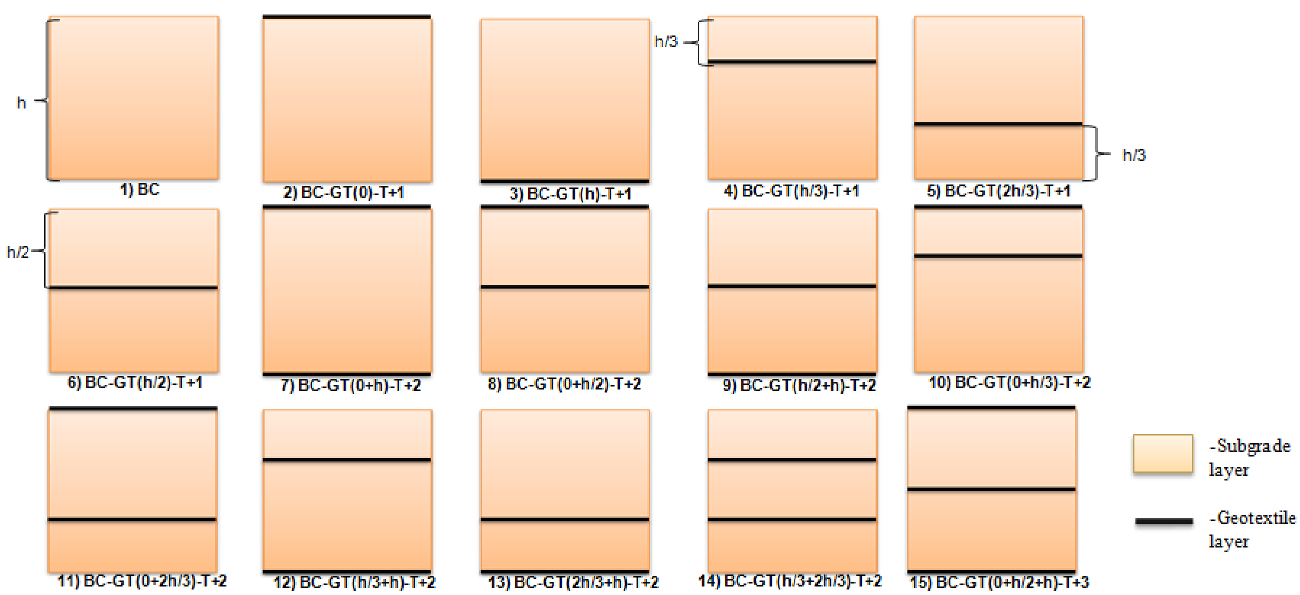

Fig.5. 1 Various Geotextile Depths considered for experimental work (h=height of apparatus of experiment)

The various specimens considered for the testing designated as BC, BC+ GT (H0+H1), BC+ GT(H0 + H2+H4), BC+ GT(H0+ H2), BC+ GT (H1), BC+ GT(H4 + H1), BC+ GT(H0 + H4), BC+ GT (H0), BC+ GT(H4 + H2) , BC+ GT (H2), BC+ GT (H0 + H3), BC+ GT (H2 + H3), BC+ GT (H4 + H3), BC+ GT (H3), BC+ GT (H4), Where BC represented for expansive soil and H0, H1, H2, H3,H4 represents Top , one third , half, two third and bottom position of geotextile layer respectively

The specimens with the Geogrid Layer are

(i) Agg + BC
(ii) Agg + BC + bottom GG
(iii) Agg + BC + top GG + top GT
(iv) Agg + BC + top GG + half GT
(v) Agg + BC + half GG + top GT
(vi) Agg + BC + half GG + half GT

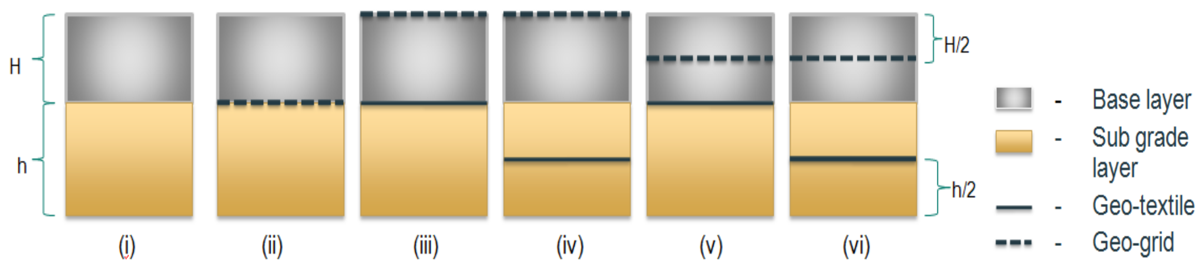

Fig.5. 2 Various Geogrid and Geotextile Depths considered for experimental work (h=height of soil layer and H is height of aggregate layer of apparatus of experiment)

Experimental analysis is done to evaluate the index properties and engineering properties of subgrade. These Properties are determined by performing three tests for different cases to be evaluated i.e. CBR (California Bearing Ratio) Test, Constant Volume Swelling Pressure Test and UCS (Unconfined Compression Strength) test which are described in the heading given below

5.1.1 CBR Test

The essential geotechnical parameter for the design of flexible pavements is California Bearing ratio (CBR) of the subgrade soil. The design method that determines the required layer thickness of the aggregate with the reinforcement in the subgrade has been based on the CBR of the subgrade soil. Since it is used to measure the strength of the subgrade soil, it is also used to assess its stiffness modulus and shear strength (Bowles 1992)

If the CBR of the subgrade is improved by providing the reinforcement, then the required thickness of the granular subbase/base layer can be reduced for a given traffic volume or, alternatively, the traffic volume can be increased for a given thickness of granular subbase/base layer

The geosynthetic reinforcement was cut in the form of a circular disk of diameter slightly less than the diameter of CBR mould. The dry weight required for filling the mould was calculated based upon the maximum dry unit weight (MDU) and the water corresponding to OMC was added in the soil and then the soil was mixed thoroughly. The mould is filled with expansive soil by placing geosynthetic reinforcement at predetermined depth as shown in Fig. 3. The cross section of the model along with the position of geosynthetic reinforcement is shown in Fig.4 . The surcharge weights were placed on the specimen to stimulate the effect of the thickness of road construction overlying the layer being tested. Constant rate(1.25mm/min) of Load is applied with the help of plunger into the soil. The value of Load observed is noted down at penetration of 0.5mm to until 12.5mm. The standard CBR tests were performed in the laboratory to compare the performance of various geosynthetics under the same subgarde soil condition.

$$C.B.R. = \left(\frac{PT}{PS}\right) \times 100$$

where,

PT = Corrected test load corresponding to the chosen penetration

PS = Standard load for the same penetration

To evaluate the bearing strength of reinforced and unreinforced soil subgrade, CBR has been conducted. The soaked CBR value for statically lightweight compact expansive soil at 95% MDD and OMC was evaluated with 4 days soaking period.

Fig.5. 3 Top view of CBR mould with Geotextile at top

5.1.2 Constant volume Swelling Pressure Test

It has been shown by several investigators that expansive soils are well known for non-uniform deformations and random movements caused by moisture content changes and in turn cause extensive damage (Chen, 1975; Nelson and Miller, 1992, and Pusch and Yong, 2006).

Swelling pressure is an important parameter for understanding the expansive nature of the natural clayey soils. During the wetting process, the intergranular stresses evolve due to the capillarity and adsorption of clay minerals, and swelling pressure is developed if soil deformation is constrained by the boundary conditions.

To investigate the swelling behavior of reinforced and unreinforced soil the constant volume swelling pressure test has been carried out. Various sections as per Fig 3 have been compacted in the 100 mm diameter 1000 cc mould. The specimen was submerged in the water for the 7 days. Load applied and heave produced in the specimen is observed with the help of Dial Gauge. Upward Swelling Pressure and heave is than calculated with the help of observed value. This test shows the Expansion and Swelling Pressure of the soil with the help of graphs.

Fig.5. 4(a) Top view of mould with Geotextile at top, (b) Test apparatus

5.1.3 Unconfined Compression Test

UCS is used widely to determine the consistency of saturated clays and other cohesive soils (Terzaghi K, Peck RB, Mesri G. Soil mechanics in engineering practice. 3d ed. New York: John Wiley and Sons; 1996. p. 512)

A cylindrical mould with a H/D ratio of about 2 and diameter of 38 mm or more is set up between end plates. Vertical Load is applied at constant rate (1.25mm/min) with the help of plates on the mould. This strain rate is so rapid as compared to drainage of sample so that is why the mould generally crack or bulge out. The load at which failure occurs is considered as unconfined compressive strength. UCS tests were performed following the American Society of Testing Materials (ASTM) D 2166-00.

The samples were prepared as per the test sections mentioned in Fig 3. The deviated stress was calculated by applying the 1.25mm/min constant strain rate up to deviator stress.

Fig.5. 5 UCS mould ready to test

5.2 Results and Discussion

Firstly, the constant swelling pressure test was conducted for soil specimen with synthetic geotextile at different depth for the placement condition of OMC at MDD and the upward swelling pressure and heave recorded by dial gauge and proving ring readings for the period of 7 days to attain the equilibrium swell. The results of the constant swelling pressure with and without synthetic geotextile layer reinforcement have been show as plot of time (logarithmic scale) versus swelling pressure in Fig.5.6.

From the plot it can be clearly noted the placement of GT at bottom do not affect much. The similar swelling pressure pattern of unreinforced and GT placed at bottom reinforced specimen. It also depicts that the swelling pressure of the GT reinforced expansive soil in almost all the cases shows minimal swelling pressure up to 120min then increments in the of upward swelling pressure has been observed. The Fig 2 shows the box plot of reinforced and unreinforced expansive soil. The figure compares the effect of GT at different stages i.e. minimum, one third, half, median, two-third and maximum of swelling pressure. From Fig 2, It can be seen that the swelling pressure of specimen BC+ GT (H0+H1),BC+ GT(H0 + H2+H4), BC+ GT(H0+ H2), BC+ GT (H1),BC+ GT(H4 + H1),BC+ GT(H0 + H4), BC+ GT (H0),BC+ GT(H4 + H2), BC+ GT (H2), BC+ GT(H0 + H3), reduced by 91.67%, 84.85%, 80.31%, 78.79%, 76.52%, 70.46% 68.95%, 68.19%, 62.89%, and 60.62% respectively. The remaining section which includes BC+ GT (H2 + H3), BC+ GT (H4 + H3), BC+ GT (H3), BC+ GT(H4) also shows reduction in upward swelling pressure by 39.41%, 34.87%, 34.11% and 1.07% respectively.

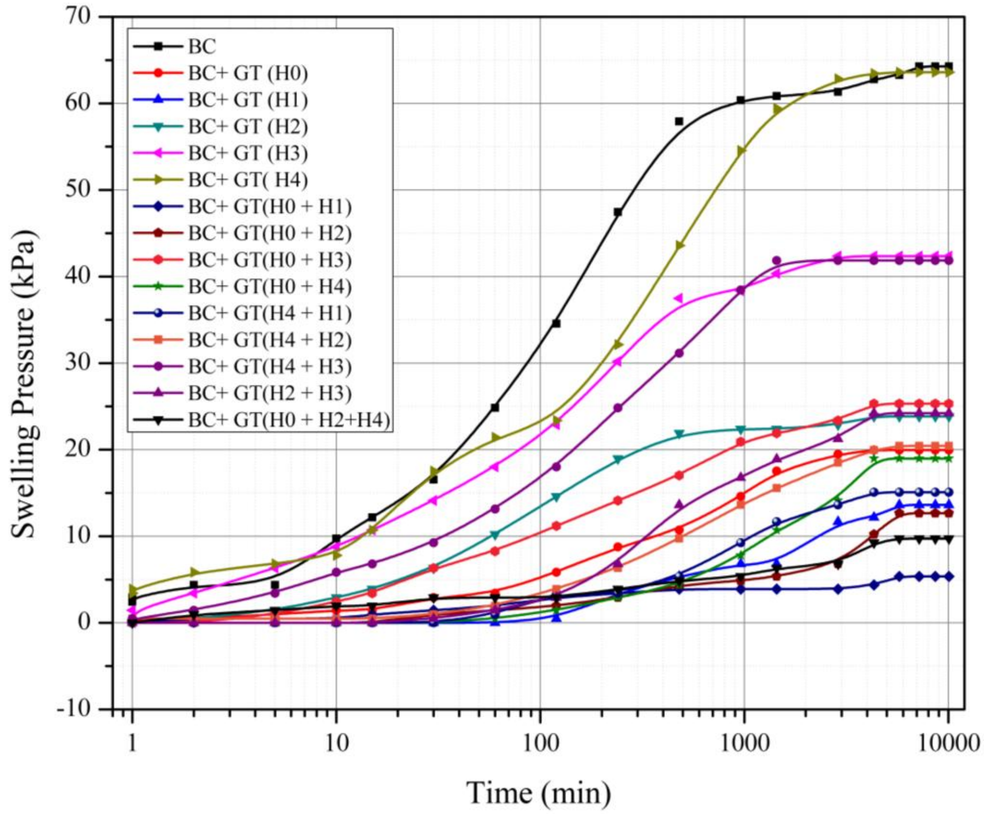

Fig.5. 6 Graph of Swelling Pressure vs time

It can also observe that placement of GT at bottom and two third depth do not significantly reduce the swelling pressure, however placement of GT at one third depth and top highly reduces the upward swelling pressure. The geotextile layer and top and one third and even at half depth intact the soil mass and the tensile strength of GT layer offered resistance against the upward swelling pressure and the exponential reduction the is observed. The confinement created by the geotextile layer reduces the migration of the soil grains and support to intact the soil mass which significantly improvise the swelling behavior of the reinforced expansive soil. The GT layer with soil mass has frictional resistance which controls the swelling pressure. The effect of bottom GT layer is not much because the majority of swelling pressure exerted half of its total height hence minimal changes observed.

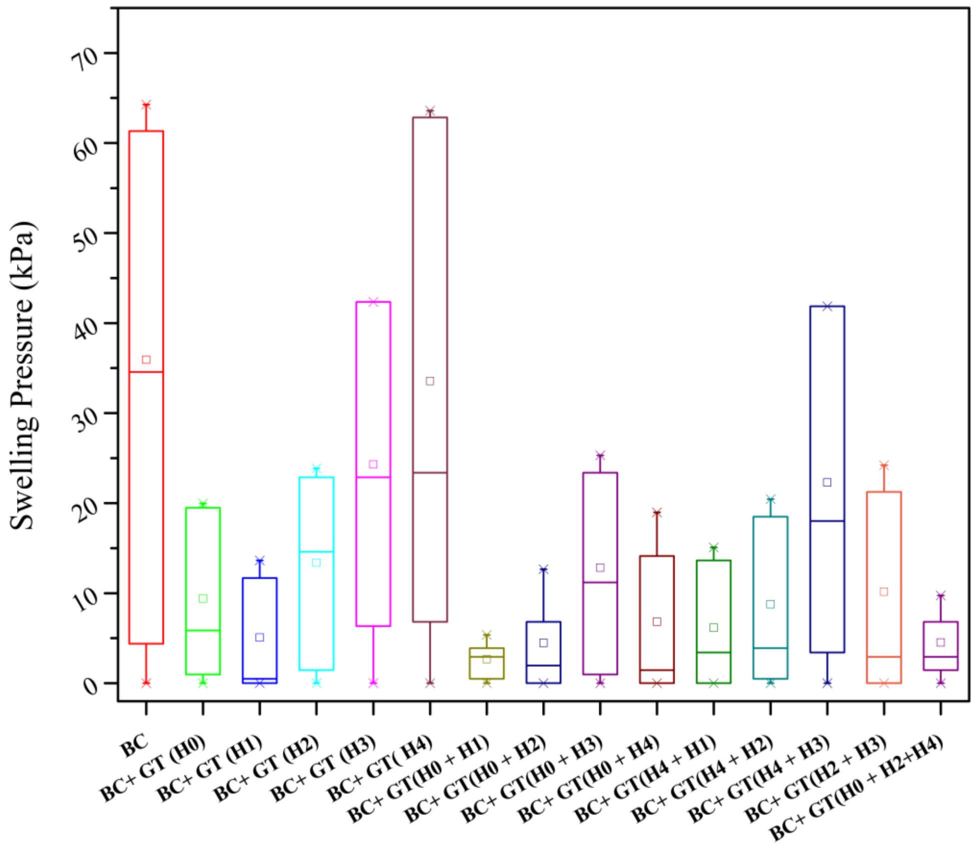

.

Fig.5. 7 Box Plot to show the variation in swelling Pressure

Figure 5.8 depicts the percentage swell with and without the synthetic geotextile layer. It shows swell in expansive soil rises exponentially without and with bottom reinforcement of GT. During the initial process, clay having air voids, and upon filling with water it develops pore pressure. As a result, the volume changes rapidly; however, after reaching the saturation limit the expansion was minimal. The reduction in the infiltration rate of water in soil mass decreases the rate of expansion per minute.

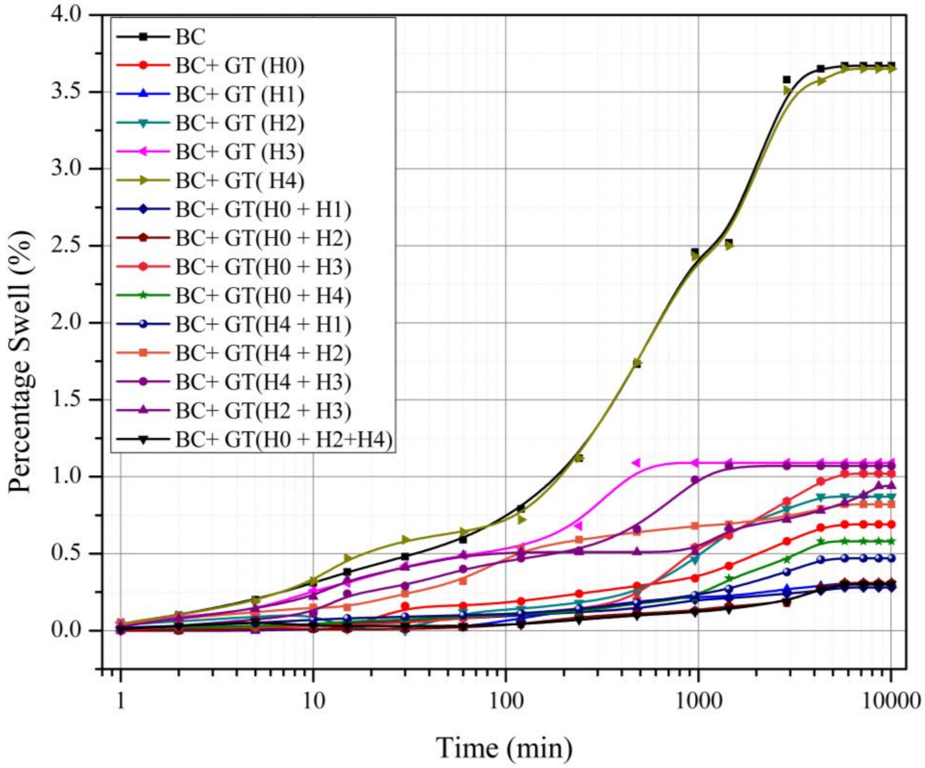

Fig.5. 8 Graph of Percentage swell for unreinforced and reinforced section

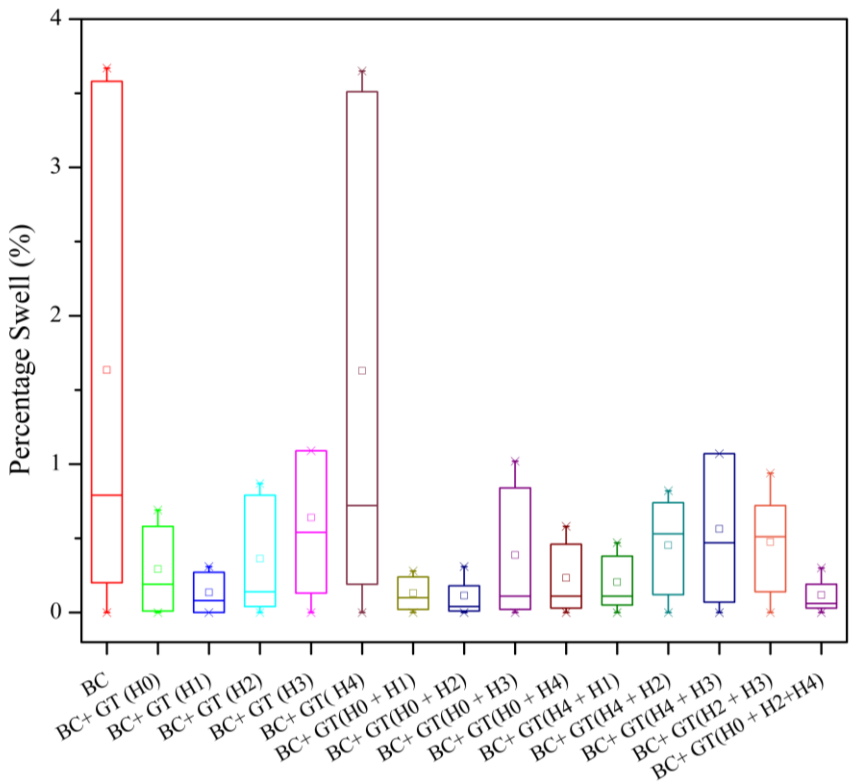

Fig.5. 9 Box plot for the percentage swell for unreinforced and reinforced section

Figure 5.10 shows the time ratio plot of swelling pressure. The plot has been plotted to explain the swelling time taken by each specimen. The given equation has been used to calculate the time ratio between reinforced and unreinforced sample to reach equilibrium condition. It can be observed that the maximum time to achieve the condition of equilibrium was of unreinforced soil sample. The BC+ GT (H4+H3) has taken very less time to achieve the condition of equilibrium.

$$T_r = \frac{T_{reinforced}}{T_{unreinforced}}$$

Where

T_r = Time ratio

$T_{reinforced}$= Time duration of maximum swelling pressure of reinforced section

$T_{unreinforced}$= Time duration of maximum swelling pressure of unreinforced section

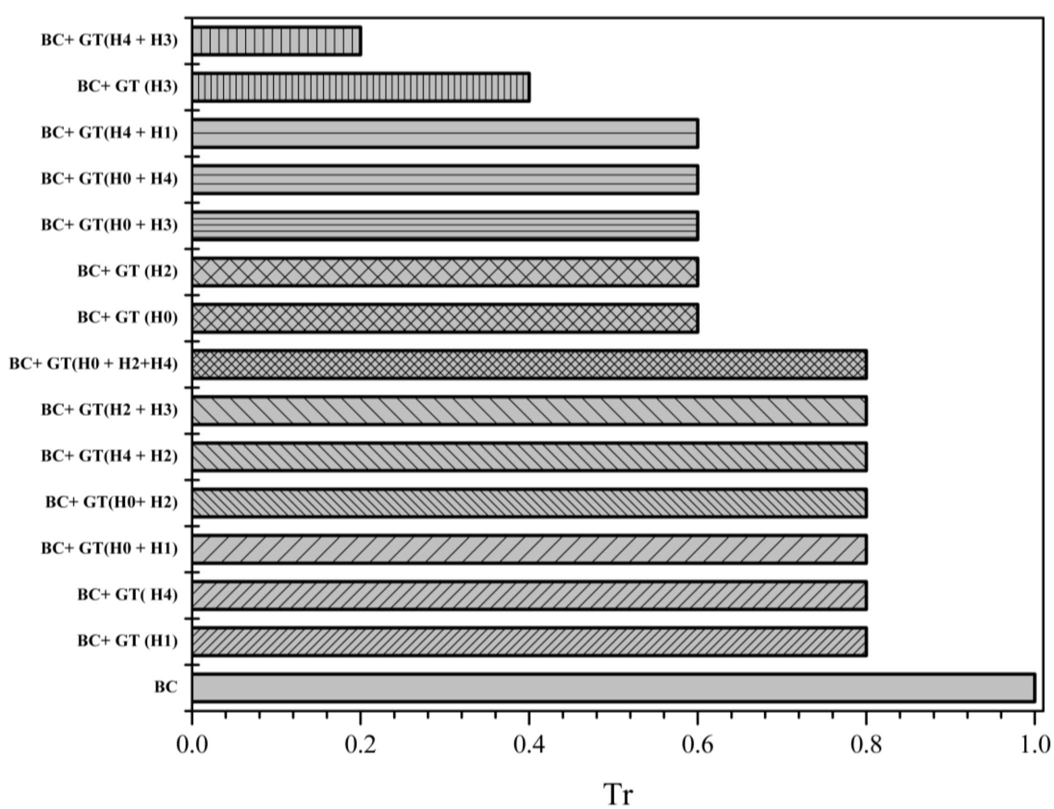

Fig.5. 10 Time ratio plot for various cases

Figure 5.11 shows the effect of geotextile layer on swelling pressure and percentage swell ratio of soil. The swelling pressure ratio (SPr) and percentage swell (PSr) calculated as per the given equations. The plot is used to evaluate clear changes in terms of ratio to better understanding about swelling pressure and percentage swell reduction. From the figure it can be noted that SP_r and PS_r is observed as 0.08 for BC + GT (H0+H1), which shows exponential reduction in the swelling pressure and percentage swell. From the Fig.5.11 it can also be noted that the swelling pressure is reduced more due to the tensile strength of the geotextile layer, however the swelling percentage are still higher than the reduction in swell pressure.

$$SP_r = \frac{SP_{reinforced}}{SP_{unreinforced}}$$

Where,

SP_r = Swelling pressure ratio; $SP_{reinforced}$= Swelling pressure of reinforced section; $SP_{unreinforced}$= Swelling pressure of unreinforced section

$$PS_r = \frac{PS_{reinforced}}{PS_{unreinforced}}$$

Where: PS_r = Percentage swell ratio; $PS_{reinforced}$= Percentage swell of reinforced section; $PS_{unreinforced}$= Percentage swell of unreinforced section

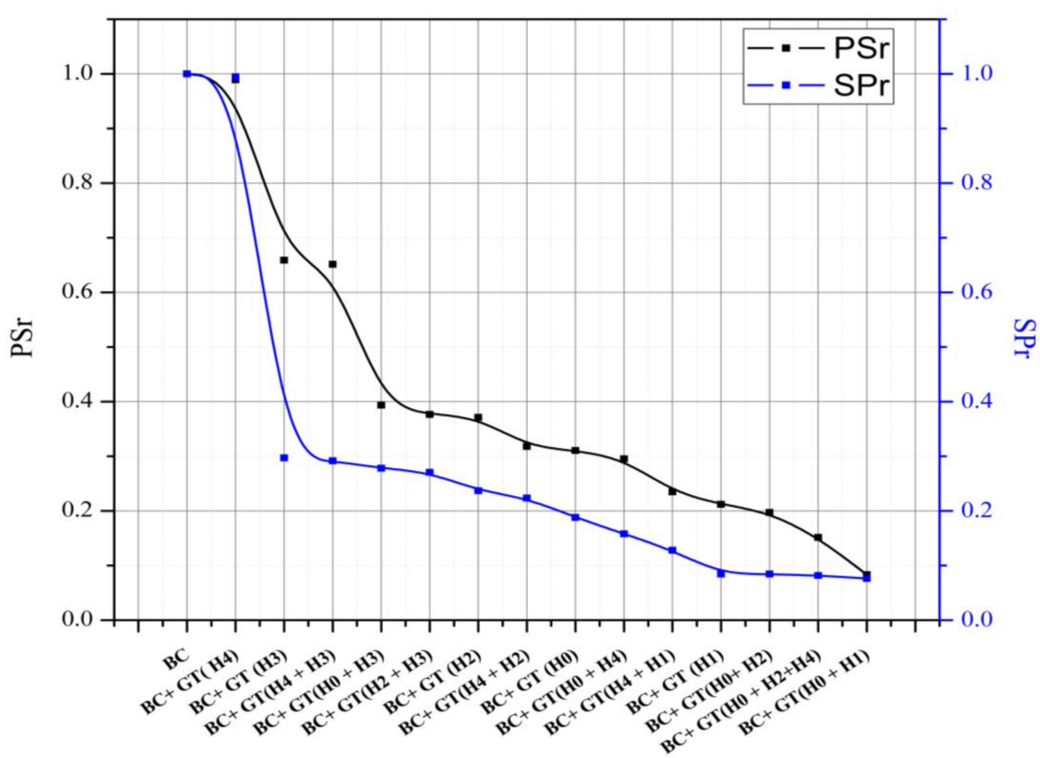

Fig.5. 11 Effect of Geotextile layer on swelling pressure and percentage swell ratio

Figure 5.12 represents the effect of synthetic geotextile on the California bearing ratio of expansive soil when Geotextile is included in the Subgrade layer. The soaked CBR of unreinforced section increases exponentially with the inclusion of GT layer. It is shown in Fig.5.12 that the CBR value at 2.5 penetration depth increases upto 5.24%. However, section BC+GT (H4), BC+GT (H3) shows similar results as unreinforced CBR value. It shows placing geotextile layer at bottom and two-third level does not affect the bearing capacity of expansive soil. However test section BC+GT(H4+H3), BC+GT(H2+H3), BC+GT(H0+H3), BC+GT(H2), BC+GT(H4+H2), BC+GT(H0), BC+GT(H0+H4), BC+GT(H4+H1), BC+GT(H1), BC+GT(H0+H2), BC+GT(H0+H2+H4), BC+GT(H0+H1) shows the CBR value as 2.13%, 2.44%, 2.68%, 2.74%, 2.97%, 3.04%, 3.26%, 3.56% , 3.98%, 4.14%, and 5.24% respectively. The range of the CBR value increase with the inclusion of geotextile layer varying from 50% to 270%. The maximum CBR value is observed at the test section BC+GT(H0+H1) since the top layer, and one-third depth of the soil specimen play an important role in the bearing capacity. The one third GT layer reduces the soil particle migration and due to intact soil mass more CBR value is observed. The geotextile layer due to its tensile strength resists the applied load and as a result the increase in the CBR value observed. The anchored geotextile layer creates diaphragm action during the CBR test and opposes the penetration. It can be noted that the value of CBR only increases up to the half depth of the soil specimen, which shows that placing the geotextile layer below half depth of the soil sample required to reinforce do not affect its bearing capacity. Single-layer geotextile and double layer geotextile both increase the CBR value up to great extent and hence can be used as the expansive soil reinforcement mechanism.

Fig.5.13 shows the effect of synthetic geotextile and Geogrid on the California bearing ratio of expansive soil and the aggregate. Geogrid is present in Base layer and Geotextile is present in subgrade layer. The soaked CBR of unreinforced section increases with the inclusion of GT and GG layer both. As shown in Fig.5.12 that the CBR value at 2.5 penetration depth is not much affected but increases with respect to unreinforced section as no geosynthetic layer is present. However, CBR of section BC+Agg+GT(Ho)+GG(ho) is 35.46%, i.e., maximum as both Geotextile and Geogrid is present at the top of respective layer. CBR of BC+Agg, BC+Agg+GG(h4), BC+Agg+GT(H2)+GG(ho), BC+Agg+GT(Ho)+GG(h2), BC+Agg+GT(H2)+GG(h2) test sections are 29.17%, 29.94%, 31.08%, 31.28% and 32.02%

respectively. The Geogrid Layer due its interlocking property holds the aggregate tight which helps in increasing the strength.

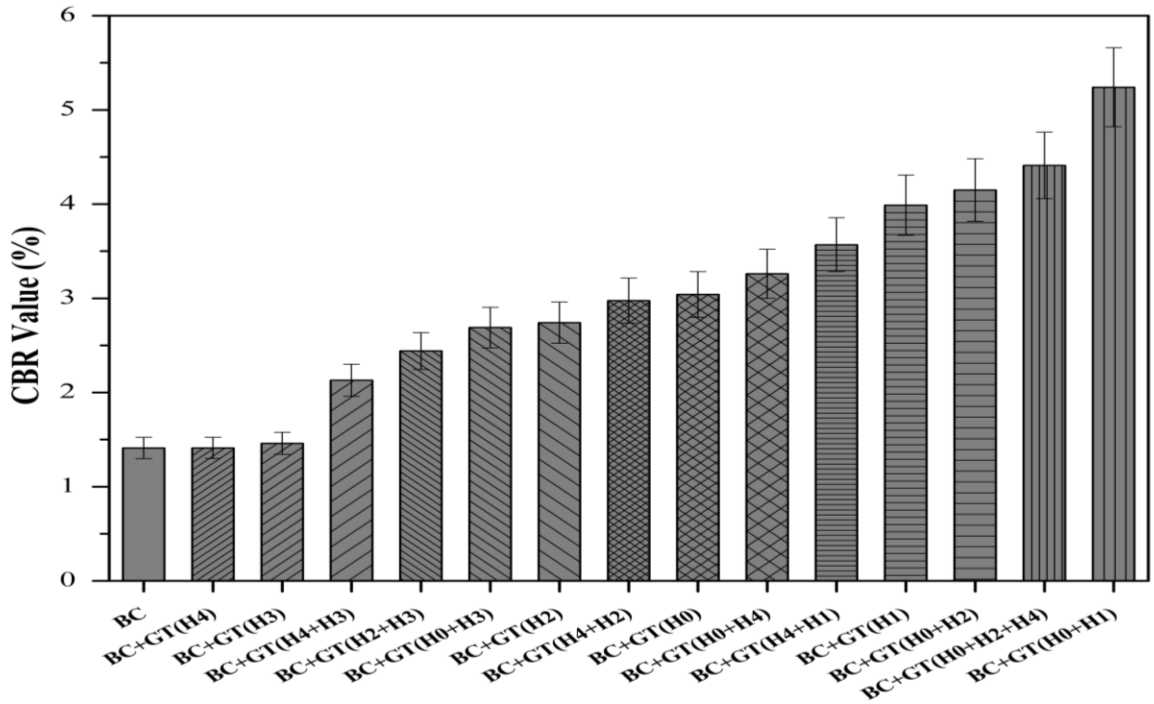

Fig.5. 12 Graph shows the change in CBR values for reinforced and unreinforced cases

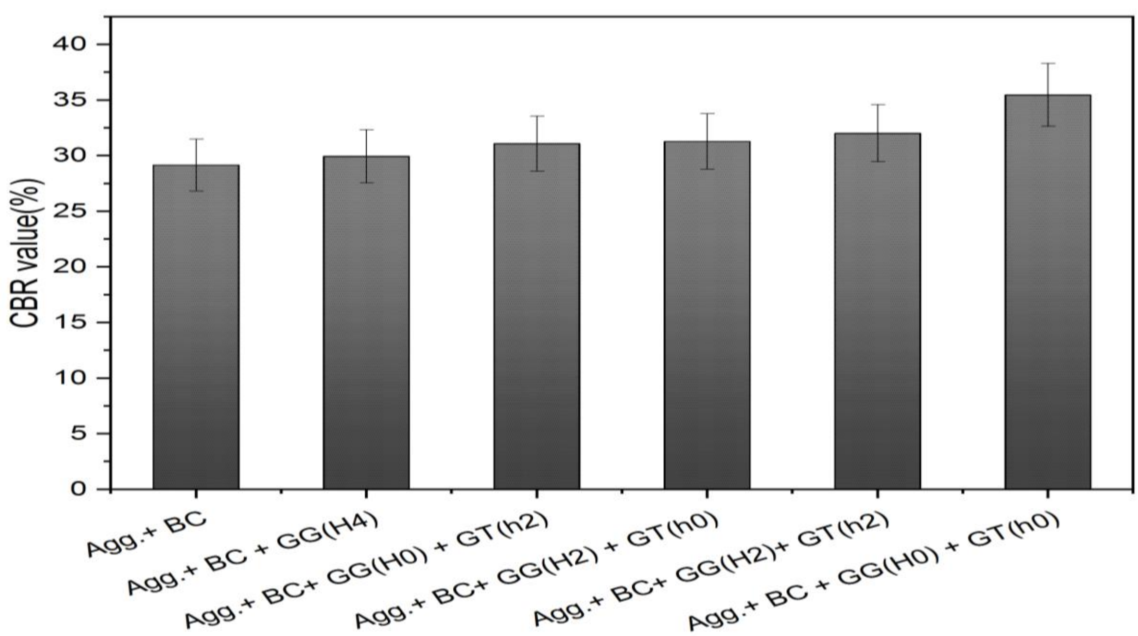

Fig.5. 13 Graph shows CBR value of unreinforced and reinforced case with Geogrid and Geotextile

The axial stress-strain curves for the expansive soil with Geotextile are shown in the Fig.5.14. The unconfined compressive strength of the expansive soil with geotextile is increased as compared to the strength of expansive soil only. As it can be seen from graph, that when only one layer is used, the compressive strength is max when geotextile is placed at one third distance from the top; when 2 layers at different positions are used, compressive strength is maximum in the case of H1+H4, i.e., when one geotextile layer is at one third from the top and another at the bottom. However, Compressive strength is maximum when expansive soil comprises of three layers, one at the top, second in the middle and another at bottom. This shows that using three layers of geotextile gives higher potential to increase the strength along with sustaining the load for large axial strain.

Fig.5.15. shows the deformation behaviour of reinforced and unreinforced expansive soil when vertical load is applied at the unconfined specimen.

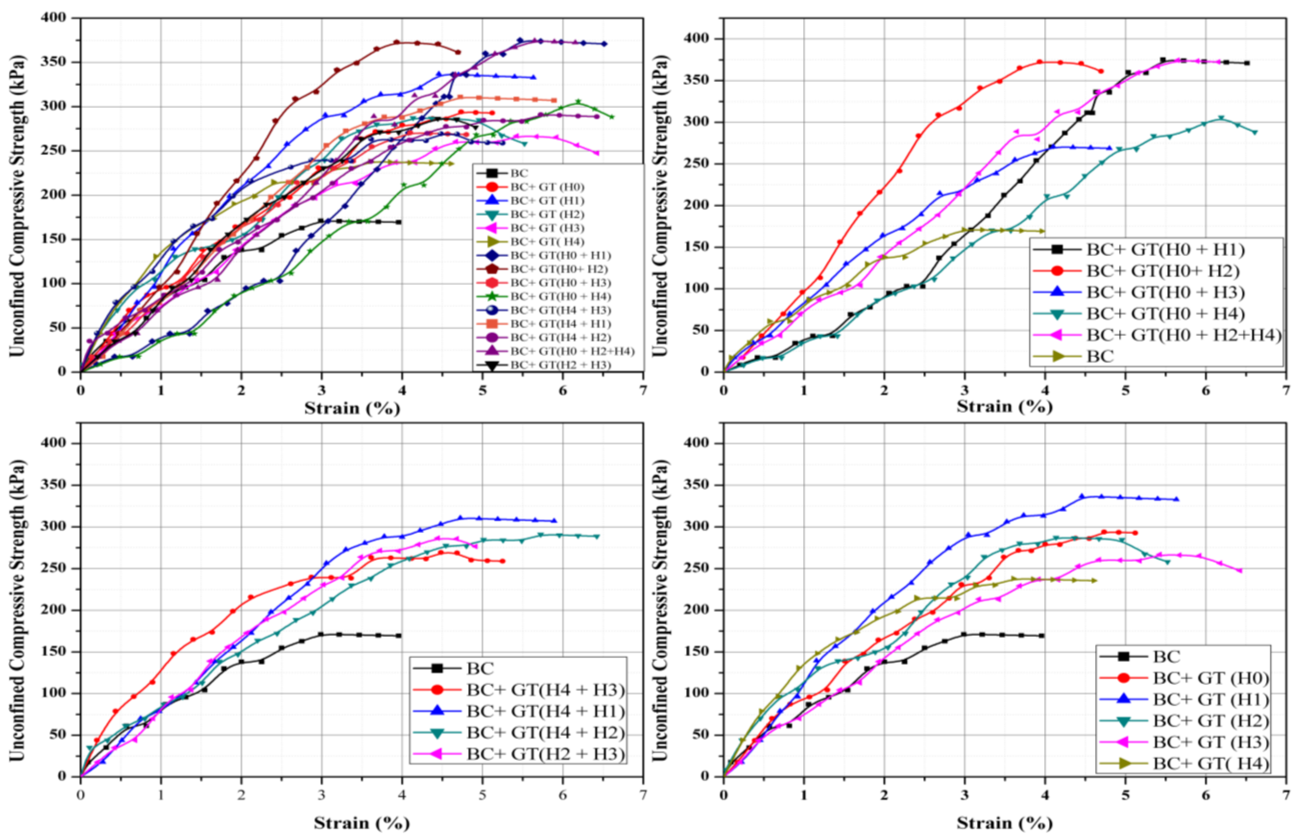

Fig.5. 14 Axial stress-strain curve of reinforced and unreinforced expansive soil

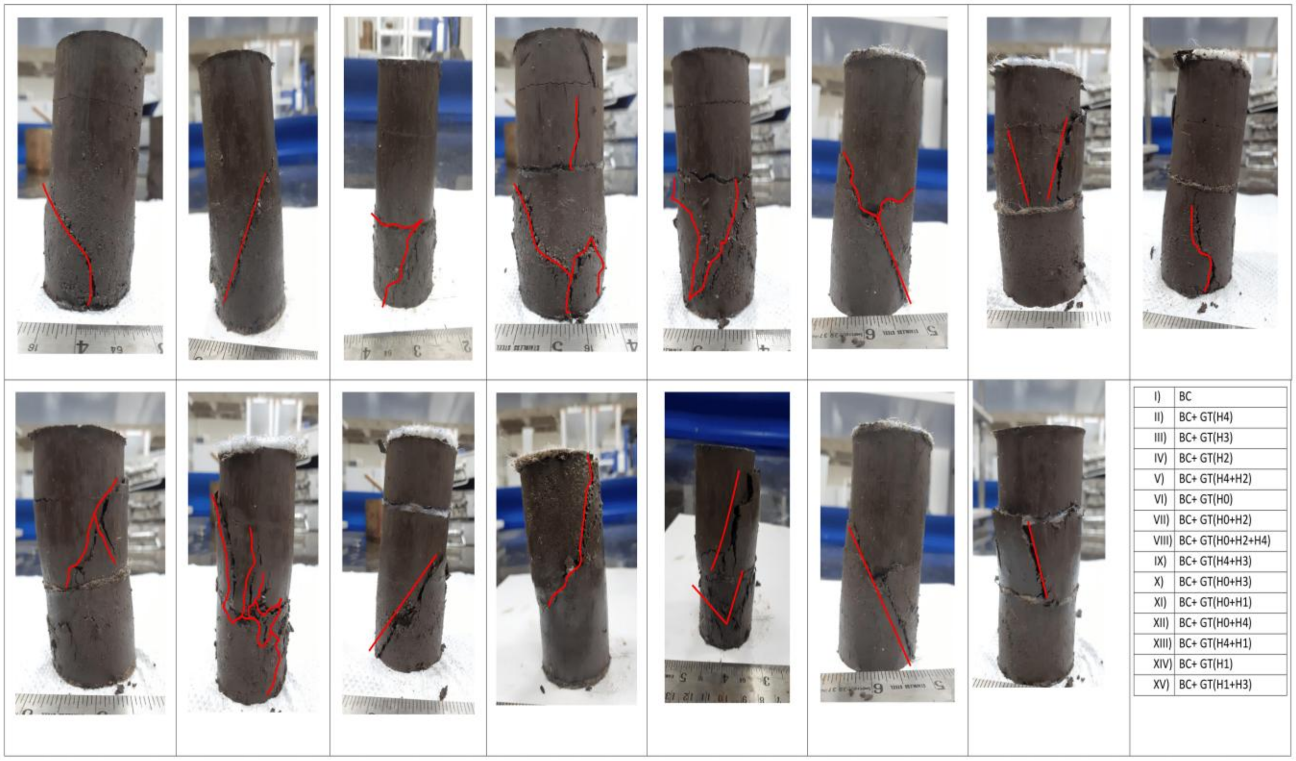

Fig.5. 15 UCS deformation behavior of reinforced and unreinforced expansive soil

Chapter 6

Numerical Performance Evaluation

Finite element analysis were conducted on a flexible pavement structure to determine the benefits of using geosynthetic like geotextile and geogrid to reinforce the base and subgrade layer. These methods are widely accepted because of their accuracy in predicting practical conditions more realistically than theoretical or analytical solutions based on the infinite slab and other idealized assumptions.

Easily available finite element software, Abaqus Unified FEA, was used in this research. Abaqus Unified FEA helps in doing more accurate simulation of expansive soil behavior using different built-in material models (Puppala el al. 2013, Chittoori et al. 2017). To solve a problem accurately in Abaqus Unified FEA, geometry, material properties, boundary conditions and interaction properties need to be established properly. This model can handle volumetric movement and the suction relationship of expansive soils with moisture variation.

The goal of the numerical analysis is to study how soils with differing swell potentials respond to various geosynthetic reinforcements. For this purpose, finite element models were developed to simulate the models that were calibrated using the laboratory data obtained from the experimental Analysis. This chapter describes the development of the numerical models, their calibration procedure and the subsequent use of these models to conduct a parametric study.

To properly represent the structur design of a flexible pavement, the geometry was modeled as a 3-D model with three pavement structural layers: subgrade soil, aggregate granular base, and Surface Layer. However, this model can be made as a 2-D model as it takes less analysis time. But 2-D model cannot simulate the real world wheel load. In this, moisture swelling model and sorption model is used to characterize the swelling nature of soils.

Important outcomes from the numerical analysis are presented, and inferences are drawn.

6.1 Geometry

The Geometry and the cross section of the model had been formed considering the pavement design. A 3.5m × 7m × 0.150m granular base layer was overlaid on a 3.5m × 7m × 0.600m expansive subgrade layer, above which lie a 3.5m × 7m × 0.100m. In this model, a Geotextile layer of dimension 3.5m × 7m × 0.0035m and Geogrid Layer of dimension 3.5m × 7m × 0.002m is modeled to use at 4 extreme positions in subgrade layer and granular base layer respectively. These four cases of numerical modeling are:

i) Agg.+ BC + GT(H0)
ii) Agg.+ BC + GT(H4)
iii) Agg. + BC + GG(h0) + GT(H0)
iv) Agg. + BC + GG(h2) + GT(H0)

Three-dimensional deformable shell element was used to develop geogrid. This element was assigned as membrane to offer strength in the plane of the surface with no bending stiffness. For the simplification of the modeling approach and computational time, geogrid was considered as geogrid membrane sheet. The inclusion of geosynthetic increases the stiffness surrounding zone of the base layer.

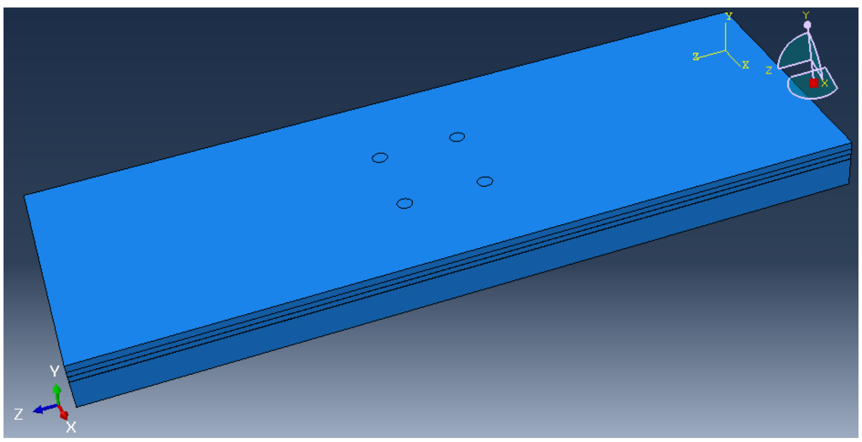

Fig 6. 1 Geometry of the model

6.2 Material Model

Next step in modeling is to assign material properties. Different Material Models were used to properly show the properties of each layer, which help in producing a comparable result on application of load.

6.2.1 Linear Elastic Model

This Model is used to simulate every layer in the model, i.e., Surface Layer, Base Layer, Subgrade Layer, Geotextile Layer and Geogrid Layer. The Modulus of the Base Material was correlated with CBR Test. The modulus of the subgrade and base material was correlated from the California Bearing Ratio (CBR) test. The correlation of CBR and resilient modulus suggested by Mechanistic-Empirical Pavement Design Guide (MEPDG) was used (Guthrie and Jackson 2015).

$$M_R = \begin{matrix} 10 * CBR & \quad for\ CBR \leq 5 \\ 17.6 * (CBR)^{0.64} & \quad for\ CBR > 5 \end{matrix}$$

Where, M_R = Resilient modulus of subgrade soil.

In this model, the total stress is defined from the total elastic strain as

$$\sigma = D^{el} \varepsilon^{el}$$

where ,

σ : total stress

D^{el} : fourth-order elasticity tensor and

ε^{el} : total elastic strain

$$\begin{Bmatrix} \varepsilon_{11} \\ \varepsilon_{22} \\ \varepsilon_{33} \\ \gamma_{12} \\ \gamma_{13} \\ \gamma_{23} \end{Bmatrix} = \begin{bmatrix} 1/E & -\nu/E & -\nu/E & 0 & 0 & 0 \\ -\nu/E & 1/E & -\nu/E & 0 & 0 & 0 \\ -\nu/E & -\nu/E & 1/E & 0 & 0 & 0 \\ 0 & 0 & 0 & 1/G & 0 & 0 \\ 0 & 0 & 0 & 0 & 1/G & 0 \\ 0 & 0 & 0 & 0 & 0 & 1/G \end{bmatrix} \begin{Bmatrix} \sigma_{11} \\ \sigma_{22} \\ \sigma_{33} \\ \sigma_{12} \\ \sigma_{13} \\ \sigma_{23} \end{Bmatrix}$$

For Isotropic case,

Shear Modulus G can be expressed as

$$G = \frac{E}{2(1+\nu)}$$

where ,

E = Young's Modulus

ν = Poisson's Ratio

These are the equations that are used to now finally the stress and strain relation in the layer as E and ν are the variables given for each layer. Inputs that are given to models for linear elasticity are as follow:

	Surface Layer	Base Layer	Subgrade layer	Geotextile	Geogrid
Young's Modulus(MPa)	454	306	135.8	392	410
Poisson's Ratio	0.3	0.35	0.4	0.35	0.3

Table.6. 1 Input values for Linear Elastic Model

6.2.2 Mohr Coulomb Model

Expansive soil contains plastic nature. So, Plastic property of subgrade material is given by Mohr Coulomb Model. This model is employed with the linear elastic model. These values are calculated with the help of shear test of soil.

$$G = \sqrt{(\varepsilon c \tan \emptyset)^2 + (R_{mw} q)^2} - pTan\varphi$$

Where

$$R_{mw}(\theta, e) = \frac{4(1-e^2)Cos^2\theta + (2e-1)^2}{2(1-e^2)\cos\theta + (2e-1\sqrt{4(1-e^2)Cos^2\theta + 5e^2 - 4e}} R_{mc}(\frac{\pi}{3}, \emptyset),$$

And

$$R_{mc}\left(\frac{\pi}{3}, \emptyset\right) = \frac{3 - \sin\emptyset}{6\cos\emptyset}$$

$$e = \frac{3 - \sin\emptyset}{3 + \sin\emptyset}$$

Where,

φ = Internal Angle of Friction

Ψ = Angle of Dilation

c = Cohesion

This model is used for subgrade layer only. The input values for this model are

	Internal Angle of friction, φ	Angle of Dilation, Ψ	Cohesion, c (kPa)
Subgrade	23.5	7.8	60

Table.6. 2 Input Values for Mohr Coulomb Model

6.2.3 Sorption Model

This model is used to define absorption and exsorption behaviors of a partially saturated medium. The sorption model illustrates the suction relationship with moisture content. This model is used for representing heaving nature of soil.

Pore pressure, uw, is used with the condition, uw ≤ 0 and the Saturation value, s lies within 0.01 ≤ s ≤ 1.Equations used in this model are:

$$u_w = \frac{1}{B} ln\left[\frac{(s - s_0)}{(1 - s_0) + A(1 - s)}\right] \; for \; s_1 \leq s < 1$$

$$u_w = u_w|_{s_1} - \frac{du_w}{ds}\bigg|_{s_1} (s_1 - s) \; for \; s_0 \leq s < s_1$$

S.No.	Pore Pressure	Saturation
1	-25	0.2
2	-15	0.3
3	12	0.4
4	-7	0.5
5	-4	0.6
6	2	0.78
7	0	1

Table.6. 3 Input values for Sorption Model

6.2.4 Moisture Swelling Model

Moisture swelling model in Abaqus Unified FEA can define the volumetric movement of soil with change in water content (Dassault Systemes 2017). Partial Volumetric saturated condition isconsidered to give volumetric swelling behavior. In this model, swelling behavior of soil is defined by

$$\varepsilon_{ii}^{ms} = r_{ii}\frac{1}{3}\left(\varepsilon^{ms}(s) - \varepsilon^{ms}(s^{I})\right)$$

Where,

$\varepsilon^{ms}(s)$ = Volumetric Swelling Strain at current Saturation

$\varepsilon^{ms}(s^{I})$ = Volumetric Swelling Strain at initial Saturation

r_{ii} = ratio allowed for anisotropic swelling

S.No.	Strain	Saturation
1	0	0.05
2	0.025	0.2
3	0.05	0.36
4	0.1	0.5
5	0.13	0.57
6	0.17	0.66
7	0.2	0.75
8	0.22	0.8
9	0.25	0.87
10	0..27	0.96
11	0.3	1

Table.6. 4 Input values for Moisture Swelling Model

6.2.5 Permeability Model

This model is used to define permeability for pore fluid flow. The above discussed two models, i.e. Sorption Model and Moisture swelling model is only applicable for the elements whose permeability model is defined.

Void Ratio = 1.53 ; K = 8E-10

6.3 Interaction Model

Interaction module is an important feature in ABAQUS especially when the model considers multi-layer system. It helps to establish the mechanical and thermal contact between the 2 layers.

The model used in this project is for the 2 layers interface is known as the surface based contact interaction. The feature of contact interaction in ABAQUS, uses the constraint approach to show the interaction between two bodies. In this feature, one surface provides a master surface which is at the top, i.e., the bottom surface of the upper layer; and other surface provides a slave surface which is at the bottom, i.e., the top surface of the lower layer. After this contact pair is defined, at each node, a family of surface contact element constructs a relative shear sliding. The interaction consists of 2 perpendicular components: Normal and Tangential to the surface.

Due to relative displacement between the layers, friction force is developed at the interface. In addition, Geosynthetiic provide tensile reinforcement and thus keep on reducing the applied vertical stress till the subgrade layer.

In this project, normal interaction was simulated by hard contact for every interaction while the shear interaction was simulated by rough contact or by specifying some friction coefficient between the contact surface pairs.

Interacting Layers (Master- Slave surface)	Interaction
Surface – Base	Penalty(0.47) + Hard Contact
Base – Subgrade	Penalty(0.47) + Hard Contact
Surface – Geogrid	Rough + Hard Contact
Geogrid – Base	Rough + Hard Contact
Base – Geogrid	Rough + Hard Contact
Base – Geotextile	Penalty(0.37) + Hard Contact
Geotextile – Subgrade	Penalty(0.37) + Hard Contact
Subgrade – Geotextile	Penalty(0.37) + Hard Contact

Table.6. 5 The different interaction condition given at the interface

6.4 Boundary Condition

Boundary Conditions were applied to replicate the control sections. Boundary Conditions were applied to the surface of each layer that are parallel to the XZ plane. These surfaces are encastred(U1 = U2 = U3 = UR1 = UR2 = UR3 = 0) which means all the nodes present in those surfaces were restricted from the movement as well as rotation in any of the three directions. These Boundary Conditions are adopted according to the design of the road.

6.5 Mesh Size

Mesh Size play an important role in finite element modeling. Appropriate knowledge on meshing approach can lead to more accurate results. Mesh Size influence greatly on the computational time also.

The mesh size of the given model is set different for the different layer as there was no significant change observed in reducing the mesh size further. Mesh size for the subgrade, base, geotextile and geogrid is set 0.15. Load is applied to the surface layer therefore mesh size for the surface layer is 0.1 and the area under pressure i.e. the area that show the print of the tire on the surface has 0.01 as the mesh size to have the more accurate result and to have the more finer stress distribution and deformation near that area.

The figures present below shows the model with the meshing for 4 different cases:

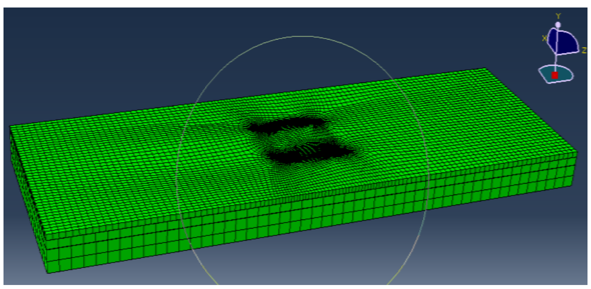

(a)

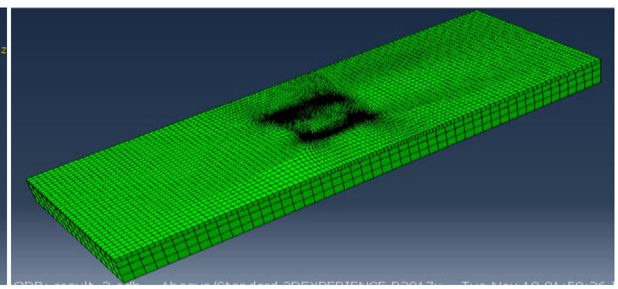

(b)

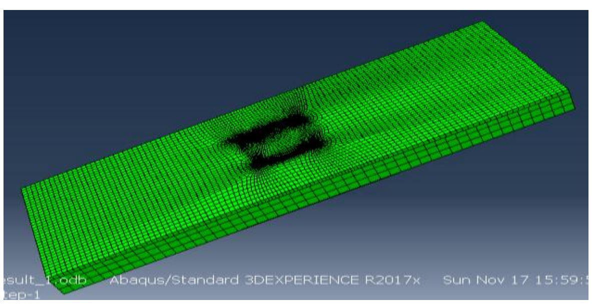

(c)

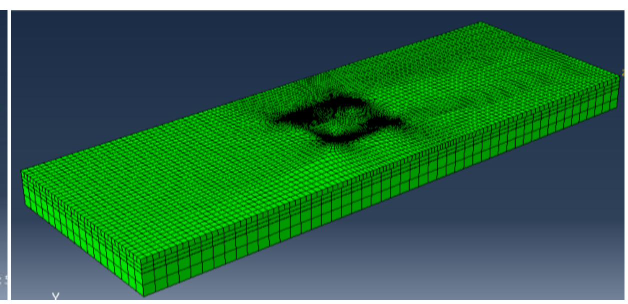

(d)

Fig 6. 2 Mesh size for (a) Agg. + BC + GG(h0) + GT(H0), (b) Agg.+ BC + GT(H0), (c) Agg.+ BC + GT(H4) and (d) Agg. + BC + GG(h2) + GT(H0)

6.6 Load Condition

The load is the necessary element in finite element modeling. Load is applied to the pavement to observe the stress strain behavior in the different layers. The wheel load was simulated by considering a circular area of diameter of 305mm (12 inch) as a print of tire on the surface of pavement section. A uniformly distributed 80kN Load, i.e., Axle load of 4 wheeler vehicle is applied on the circular area.

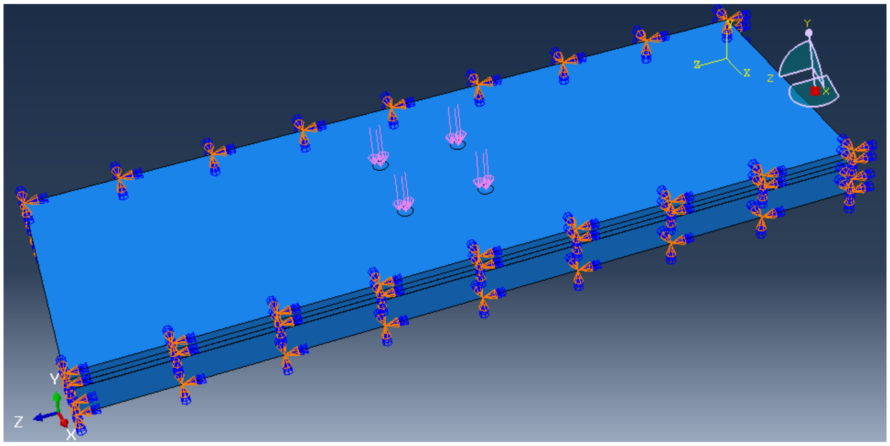

Fig 6. 3 Model after applying Load and Boundary Conditions

6.7 Validating Deformation Behavior

The main objective of numerical analysis is to simulate the flexible pavement with reinforced and unreinforced subgrade and base layer and then to check that the heave or the deformation is in permissible range or not, according to IRC 37:2012. Material Properties, Boundary Conditions and interactions that are obtained experimentally are used to form and simulate the numerical model. These conditions are similar to the actual scenario of the flexible pavement road with the vehicular load applied on it.

Stress And Strain relation obtained in the simulation can be seen in the graphs present below. The figure.6.5 and figure.6.6 also shows the stress and strain distribution in base and subgrade layer for all the cases.

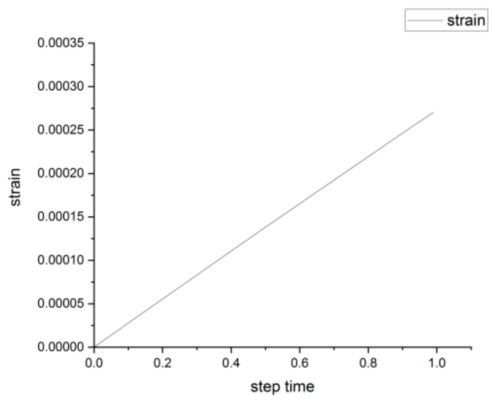

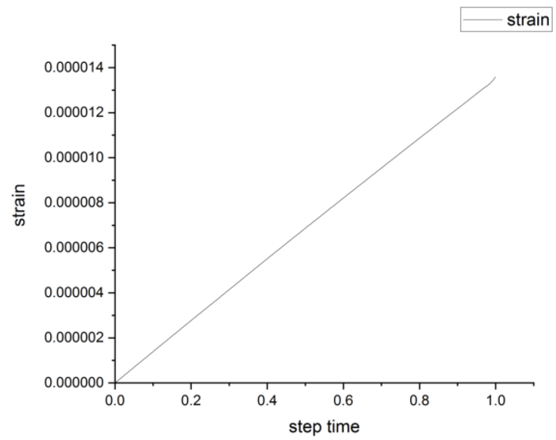

(a) (b)

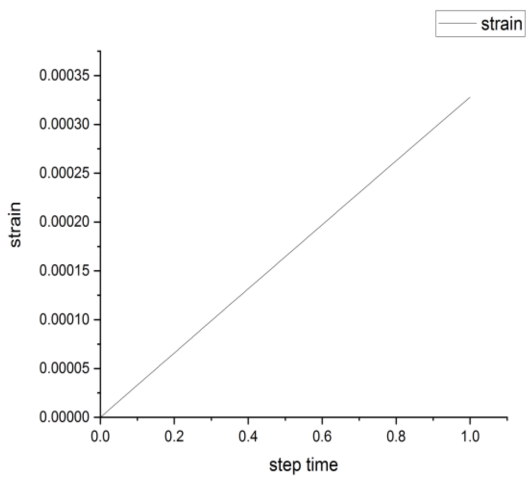

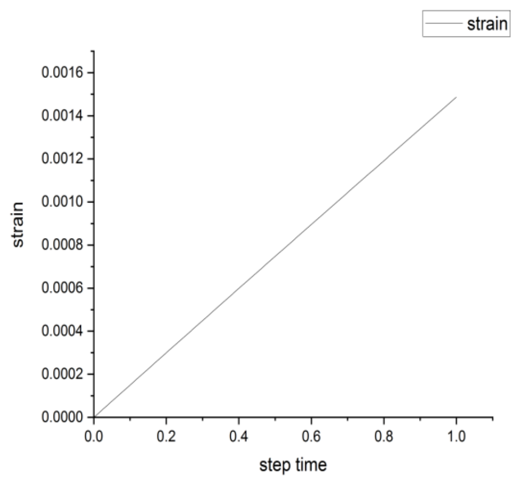

(c) (d)

Fig 6. 4 Strain vs time Graph of (a) Agg. + BC + GG(h2) + GT(H0), (b) Agg. + BC + GG(h0) + GT(H0), (c) Agg.+ BC + GT(H4) and (d) Agg. + BC + GT(H0)

According to IRC 37:2012, the limiting length of deformation for any layer is 20mm, i.e. Deformation due to rutting should be less than 20mm. Subgrade having deformation more than 20mm is not acceptable as the life of the pavement will be very less.

The results obtained for the reinforced and unreinforced pavement confirms that the deformation for each extreme case will be less than 20mm. As the strain obtained is so less in every layer that even after multiplying the height of the layer the deformation results in value less than 20mm.

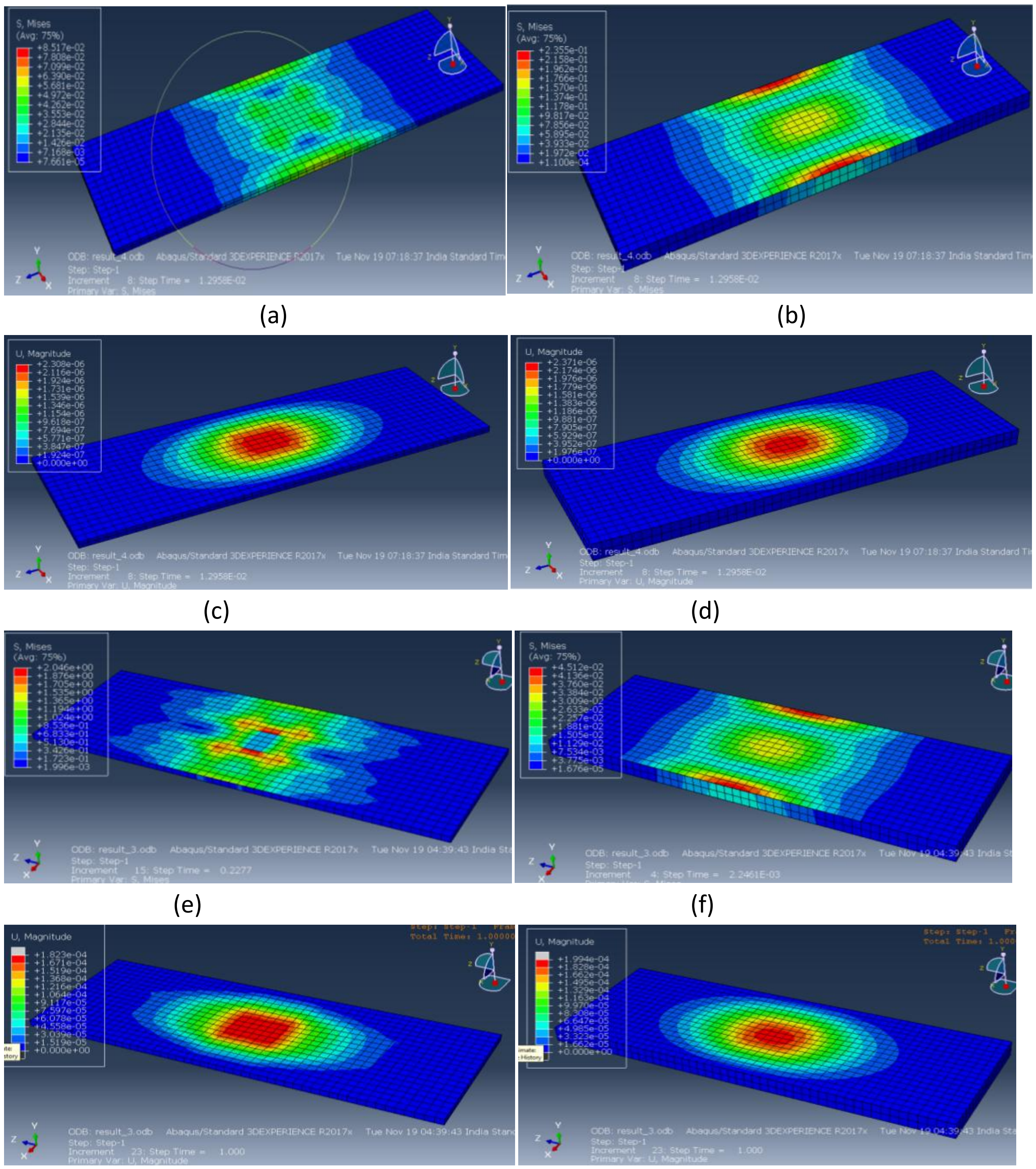

(a) (b) (c) (d) (e) (f) (g) (h)

Fig 6. 5(a),(b),(e),(f) shows the stress distribution and (c),(d),(g),(h) shows the strain distribution of base layer and subgrade layer for case(a) Agg. + BC + GG(h2) + GT(H0), (b) Agg. + BC + GG(h0) + GT(H0) respectively

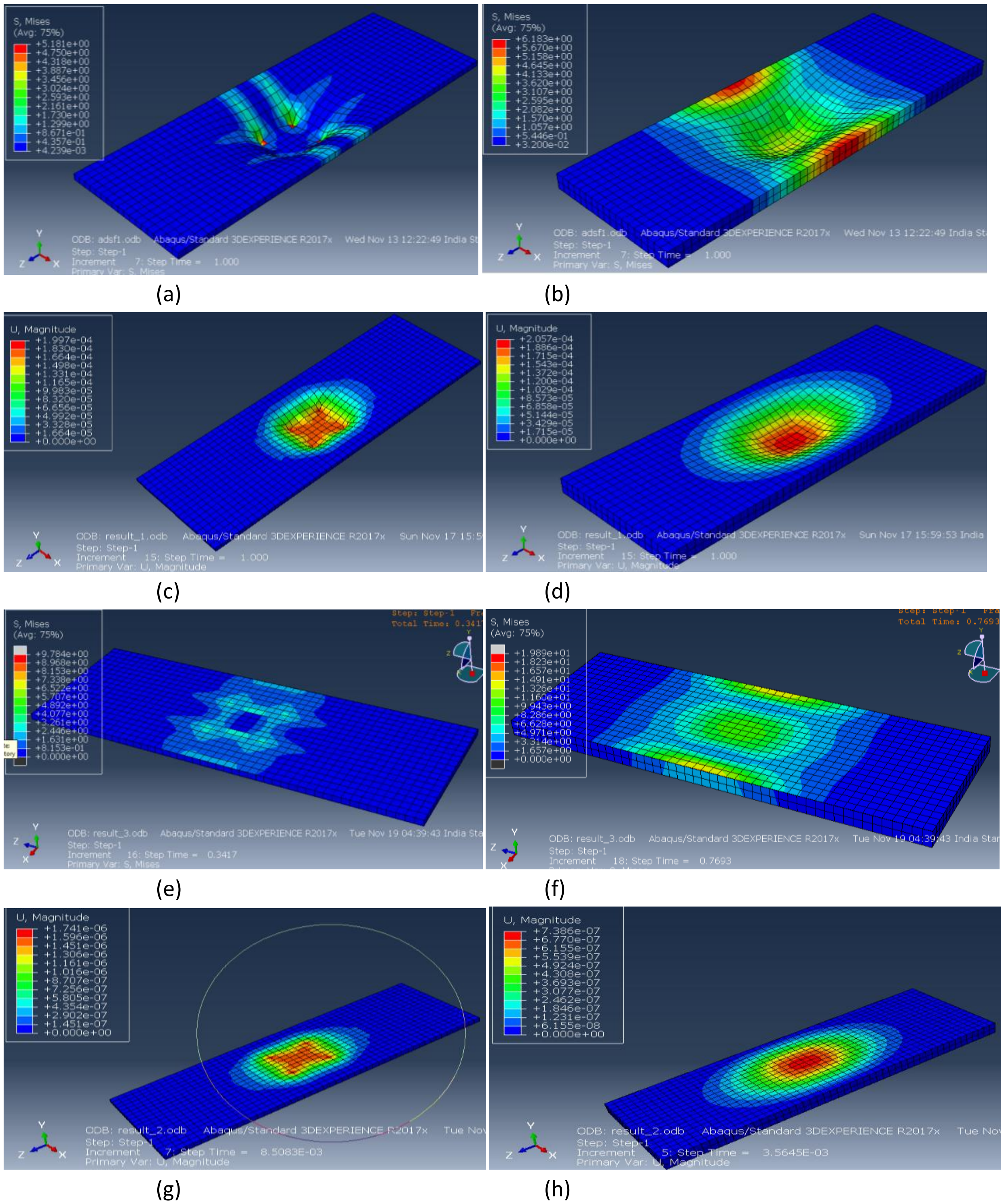

Fig 6. 6(a),(b),(e),(f) shows the stress distribution and (c),(d),(g),(h) shows the strain distribution of base layer and subgrade layer for case(a)Agg.+ BC + GT(H4) and (b) Agg. + BC + GT(H0)

Chapter 7

Result and Validation for Rutting Failure

Experimental results are analyzed and its stress, strain are observed for different cases . After that, Numerical results are obtained in which the stress and strain distribution is observed in subgrade and base layer. Now, to validate that the experimental result will give same response as shown in numerical modeling, we use this rutting formula. The equation for rutting for 90 per cent reliability is given below:

$$N = 1.41 \times 10^{-8}\left[{}^{1}/_{\varepsilon_v}\right]^{4.5337}$$

where,

N = No. of Repetition of axle Load

ε_v = Elastic Vertical Strain

The above equation is used for controlling rutting in subgrade as well as base layer.

To validate that the experimental result will give same response as shown in numerical modeling, we use this rutting formula. To find the final convergence between numerical result and experimental result, experimentally obtained N value is compared with the optimum value obtained by Numerical analysis. Experimental Vertical strain is acquired experimentally with the help of UCS test done. The maximum vertical strain obtained from the graph of strain vs time is taken as the numerical vertical strain which is then used to find the N value numerically.

The table shown below shows the comparison between the Numerically obtained N value and experimental N value.

Cases	ε_v		N		Error %
	Experimental	Numerical	Experimental	Numerical	
GG(h2)+GT(0)	3.64E-4	3.2E-4	2.98E6	3.48E6	14
GG(0)+GT(0)	1.45E-5	1.35E-5	4.76E6	6.02E6	21
GT(H)	3.38E-4	3.3E-4	2.33E6	3.03E6	23
GT (0)	9.15E-5	1.49E-4	1.02E6	1.12E6	9

Table.7. 1 Experimental and Numerical Values for subgrade Layer

This table shows that there is some error between numerical and experimental value of N. These error shows that the values which we obtained as a numerical result may vary upto that extent on the field.

The results shows that, the application of geosynthetic reinforcement placed above weak subgrade of expansive soil can markedly improved the performance by reducing the vertical deformations which results in increase in pavement service life.

Chapter 8

Conclusion and Future Work

8.1 Conclusion

The synthetic geotextile and Geogrid shows a significant improvement in the property of expansive soil subgrade. The results of the study on the potential use of synthetic geotextile to reduce the shrink-swell potential and increase the strength of expansive soils are analyzed. The results shows that reinforced soil can be used for controlling the swelling-shrinkage, bearing capacity and stress strain behaviour of the expansive soil subgrade. Based on the results already presented, the following conclusions were made

1. The expansive soils using synthetic geotextile can be used for controlling the swelling pressure of the expansive soil subgrade. It has been observed that the upward swelling pressure is reduced to approximately 91% with Geotextile. However, the placement of the geotextile at bottom influence the results less.

2. The inclusion of geotextile layer improves the CBR value due to tensile strength of coir geotextile. The CBR value has been increased to the range of 50% to 270% and the maximum CBR value is observed at the test section BC+GT(H0+H1), which can significantly reduce the thickness of the sub-base and base course of paved structure.

CBR Value is also increased by using Geogrid in base layer and geotextile in subgrade layer by approximately 13%.

3. The unconfined compressive strength of the geotextile reinforced section improved significantly. The higher value obverse when placed at top and half depth of the specimen. Since geotextile layer having higher tensile strength, which significantly influence the unconfined compressive strength of the expansive soil .

According to numerical results, we can conclude that the strain is least in case of geotextile and geogrid at top, while its least when Geotextile is placed at bottom. According to the MoRTH the deformation for rutting is 20mm, which means vertical deformation should be less than 20mm, and it is easily interpreted from the results that the deformation in these cases are less than 20mm.

The error convergence between experimental and numerical results is also in permissible range as it shows that there will be little error between the results which we obtain according to software and results which can be seen on field with the same condition. This error might be occurring due to software properties or because of manual error on field.

8.2 Future Work

Based on the findings which we have obtained from this research, there are still some suggestions for the future research efforts such as:

i) Determining the influencing factor that contributes in the improvement of base and subgrade layer.

ii) Developing a finite element model with the different moving loads which represent a large number of moving vehicles.

iii) There is a need to verify the findings of this study by developing model for full scale geotextile or geogrid reinforced structure.

Publications

1. N. Tiwari, D. Sharma and N. Satyam; Effect of Synthetic Geotextile on Swelling Pressure and Bearing Capacity Attributes of Expansive Soil Subgrade: An Experimental Study – (Journal paper, to be submitted)
2. N. Tiwari, D. Sharma and N. Satyam; Experimental Study on Swelling attributes of synthetic geotextile reinforced expansive soil – 36th International Geological Congress, New Delhi, India. (Abstract Accepted)

References

1. Akinwumi, I.I., Booth, C.A., 2015. Experimental insights of using waste marble fines to modify the geotechnical properties of a lateritic soil. J. Environ. Eng. Landsc. Manag. 23, 121–128. https://doi.org/10.3846/16486897.2014.1002843
2. Akinwumi, I.I., Ukegbu, I., 2015. Soil modification by addition of cactus mucilage. Geomech. Eng. 8, 649–661. https://doi.org/10.12989/gae.2015.8.5.649
3. Barazi Jomoor, N., Fakhri, M., Keymanesh, M.R., 2019. Determining the optimum amount of recycled asphalt pavement (RAP) in warm stone matrix asphalt using dynamic creep test. Constr. Build. Mater. 228, 116736. https://doi.org/10.1016/j.conbuildmat.2019.116736
4. Camacho-Tauta, J., Reyes-Ortiz, O., Fonseca, A.V. Da, Rios, S., Cruz, N., Rodrigues, C., 2016. Full-scale Evaluation in a Fatigue Track of a Base Course Treated with Geopolymers. Procedia Eng. 143, 18–25. https://doi.org/10.1016/j.proeng.2016.06.071
5. Consoli, N.C., Lopes, L. da S., Prietto, P.D.M., Festugato, L., Cruz, R.C., 2011. Variables Controlling Stiffness and Strength of Lime-Stabilized Soils. J. Geotech. Geoenvironmental Eng. 137, 628–632. https://doi.org/10.1061/(ASCE)GT.1943-5606.0000470
6. Correia, N.S., Zornberg, J.G., 2016. Mechanical response of flexible pavements enhanced with Geogrid-reinforced asphalt overlays. Geosynth. Int. 23, 183–193. https://doi.org/10.1680/jgein.15.00041
7. Criado, M., Fernández-Jiménez, A., Palomo, A., 2007. Alkali activation of fly ash: Effect of the SiO2/Na2O ratio. Microporous Mesoporous Mater. 106, 180–191.
8. https://doi.org/10.1016/j.micromeso.2007.02.055
9. Cristelo, N., Vieira, C.S., De Lurdes Lopes, M., 2016. Geotechnical and Geoenvironmental Assessment of Recycled Construction and Demolition Waste for Road Embankments. Procedia Eng. 143, 51–58. https://doi.org/10.1016/j.proeng.2016.06.007

10. Estabragh, A.R., Rafatjo, H., Javadi, A.A., 2014. Treatment of an expansive soil by mechanical and chemical techniques. Geosynth. Int. 21, 233–243. https://doi.org/10.1680/gein.14.00011
11. Farmer, V.C. (Ed.), 1974. The Infrared Spectra of Minerals. Mineralogical Society of Great Britain and Ireland, Londan. https://doi.org/10.1180/mono-4
12. Hammouri, N.A., Husein Malkawi, A.I., Yamin, M.M.A., 2008. Stability analysis of slopes using the finite element method and limiting equilibrium approach. Bull. Eng. Geol. Environ. 67, 471–478. https://doi.org/10.1007/s10064-008-0156-z
13. Jones, L.D., Survey, B.G., Jefferson, I., 1998. Expansive Soils, in: Institution of Civil Engineers Manuals Series. ICE Manuals, pp. 1–46.
14. Kermani, B., Xiao, M., Stoffels, S.M., Qiu, T., 2018. Reduction of subgrade fines migration into subbase of flexible pavement using geotextile. Geotext. Geomembranes 46, 377–383. https://doi.org/10.1016/J.GEOTEXMEM.2018.03.006
15. Krause Sternberg, M., 1977. DIURETIKA II. Monatskurse fur die Arztl. Fortbildung. https://doi.org/10.1016/j.trgeo.2015.06.003
16. Marradi, A., Pinori, U., Betti, G., 2012. The Use of Lightweight Materials in Road Embankment Construction. Procedia - Soc. Behav. Sci. 53, 1000–1009. https://doi.org/10.1016/j.sbspro.2012.09.949
17. Mazzoni, G., Stimilli, A., Cardone, F., Canestrari, F., 2017a. Fatigue, self-healing and thixotropy of bituminous mastics including aged modified bitumens and different filler contents.

    9. https://doi.org/10.1061/9780784412121.135
18. Constr. Build. Mater. 131, 496–502. https://doi.org/10.1016/j.conbuildmat.2016.11.093
19. Mazzoni, G., Virgili, A., Canestrari, F., 2017b. Influence of different fillers and SBS modified bituminous blends on fatigue, self-healing and thixotropic performance of mastics. Road Mater. Pavement Des. https://doi.org/10.1080/14680629.2017.1417150
20. Mounes, Sina Mirzapour, Karim, M.R., Mahrez, A., Khodaii, A., 2011. An overview on the use of geosynthetics in pavement structures. Sci. Res. Essays 6, 2251–2258.
21. Mounes, S M, Karim, M.R., Mahrez, A., Khodaii, A., 2011. An overview on the use of geosynthetics in pavement structures. Sci. Res. Essays 6, 2234–22418.

22. Nejad, F.M., Noory, A., Toolabi, S., Fallah, S., 2008. Effect of using geosynthetics on reflective crack prevention. Geotext. Geomembranes 16, 1–8. https://doi.org/10.1080/10298436.2014.943128
23. Onur, M.I., Tuncan, M., Evirgen, B., Ozdemir, B., Tuncan, A., 2016. Behavior of Soil Reinforcements in Slopes. Procedia Eng. 143, 483–489. https://doi.org/10.1016/j.proeng.2016.06.061
24. Palmeira, E.M., Bathurst, R.J., Stevenson, P.E., Zornberg, J.G., 2009. Advances in Geosynthetics Materials and Applications for Soil Reinforcement and Environmental Protection Works. Electron. J. Geotech. Eng. 38.
25. Peng, X., Zornberg, J.G., 2017. Evaluation of Load Transfer in Geogrids for Base Stabilization Using Transparent Soil, in: Transportation Geotechnics and Geoecology. pp. 307 – 314. https://doi.org/10.1016/j.proeng.2017.05.049
26. Perkins, S.W., Ismeik, M., 1997. A synthesis and evaluation of geosynthetic-reinforced base layers in flexible pavements: Part II. Geosynth. Int. https://doi.org/10.1680/gein.4.0107
27. Petry, T.M., Armstrong, J.C., 1989. Stabilization of expansive clay soils. Transp. Res. Rec. 103–Phanikumar, B.R., Nagaraju, T. V., 2018. Effect of Fly Ash and Rice Husk Ash on Index and Engineering Properties of Expansive Clays. Geotech. Geol. Eng. 36, 3425–3436. https://doi.org/10.1007/s10706-018-0544-5
28. Phanikumar, B.R., Singla, R., 2016. Swell-consolidation characteristics of fibre-reinforced expansive soils. Soils Found. 56, 138–143. https://doi.org/10.1016/j.sandf.2016.01.011
29. Punthutaecha, K., Puppala, A.J., Vanapalli, S.K., Inyang, H., 2006. Volume Change Behaviors of Expansive Soils Stabilized with Recycled Ashes and Fibers. J. Mater. Civ. Eng. 18, 295–306. https://doi.org/10.1061/(ASCE)0899-1561(2006)18:2(295)
30. Robertson, A.H.J., Hill, H.R., Main, A.M., 2013. Analysis of Soil in the Field using portable FTIR, in: Soil Spectroscopy: The Present and Future of Soil Monitoring. pp. 1–20.
31. Samer, D., Jeong, H.O., Mijia, Y., Ilias, M., Lee, S.I., Freeman, T., Mark, B., Jao, M., 2012. Pavement repair strategies for selected distresses in FM roadways. Austin, Texas.

32. Sharma, M., Satyam, N., Reddy, K.R., 2019. Investigation of various gram-positive bacteria for MICP in Narmada Sand, India. Int. J. Geotech. Eng. 1–15. https://doi.org/10.1080/19386362.2019.1691322
33. Shukla, R.P., Parihar, N.S., Gupta, A.K., 2018. Stabilization of Expansive Soil Using Potassium Chloride. Stavební Obz. - Civ. Eng. J. 27, 25–33. https://doi.org/10.14311/cej.2018.01.0003
34. Sivapullaiah, P., Sitharam, T., Subba Rao, K., 1987. Modified Free Swell Index for Clays. Geotech. Test. J. 10, 80. https://doi.org/10.1520/GTJ10936J
35. Srivastava, D.K., Srivastava, A., Misra, A.K., Sahu, V., 2018. Sustainability assessment of EPS-geofoam in road construction: a case study. Int. J. Sustain. Eng. 00, 1–8. https://doi.org/10.1080/19397038.2018.1508319
36. Mir Md. Tamim, 2017. Evaluating the effectiveness of a hybrid geosynthetic reinforcement system to mitigate differential heave on flexible pavement due to expansive subgrades
37. Sun, S., Liu, B., Wang, T., 2018. Improvement of Expansive Soil Properties Using Sawdust. J. Solid Waste Technol. Manag. 44, 78–85. https://doi.org/10.5276/jswtm.2018.78
38. Thirumalai, R., Babu, S.S., Naveennayak, V., Nirmal, R., Lokesh, G., 2017. A Review on Stabilization of Expansive Soil Using Industrial Solid Wastes. Engineering 09, 1008–1017. https://doi.org/10.4236/eng.2017.912060
39. Tinoco, J., António Alberto Santos, C., Da Venda, P., Correia, A.G., Lemos, L., 2016. A Data-driven Approach for qu Prediction of Laboratory Soil-cement Mixtures. Procedia Eng. 143, 566–573. https://doi.org/10.1016/j.proeng.2016.06.073
40. Tiwari, N., Satyam, N., 2019. Experimental Study on the Swelling Behavior of Expansive Soil Reinforced with Coir Geotextile, in: Indian Geotechnical Conference. Surat, India, pp. 1–11.
41. V, R.J. and J., 2017. A STUDY ON STABILIZATION OF EXPANSIVE SOIL USING 4, 110–120.
42. Vieira, C.S., Pereira, P.M., 2016. Interface shear properties of geosynthetics and construction and demolition waste from large-scale direct shear tests. Geosynth. Int. https://doi.org/10.1680/jgein.15.00030

43. Zornberg, J.G., 2017. Functions and Applications of Geosynthetics in Roadways. Procedia Eng. 189, 298–306. https://doi.org/10.1016/j.proeng.2017.05.048
44. Zornberg, J.G., 2012. Geosynthetic-reinforced Pavement Systems, in: 5th European Geosynthetics Congress. Valencia, pp. 49–61.
45. Zornberg, J.G., Azevedo, M., Sikkema, M., Odgers, B., 2017. Geosynthetics with enhanced lateral drainage capabilities in roadway systems. Transp. Geotech. https://doi.org/10.1016/j.trgeo.2017.08.008
46. Zornberg, J.G., Roodi, G.H., Ferreira, J., Gupta, R., 2012. Monitoring Performance of Geosynthetic-Reinforced and Lime-Treated Low-Volume Roads under Traffic Loading and Environmental Conditions, in: ASCE Geo-Congress. American Society of Civil Engineers (ASCE), Oakland, California, pp. 1310–1319. https://doi.org/10.1061/9780784412121.135